Seismic deformation analysis of Tuttle Creek Dam

Timothy D. Stark, Michael H. Beaty, Peter M. Byrne, Gonzalo Castro, Francke C. Walberg, Vlad G. Perlea, Paul J. Axtell, John C. Dillon, William B. Empson, and David L. Mathews

Abstract: To facilitate the design of seismic remediation for Tuttle Creek Dam in east central Kansas, a seismic finite difference analysis of the dam was performed using the software FLAC and the UBCSAND and UBCTOT soil constitutive models. The FLAC software has a key advantage because it can use calibrated site-specific constitutive models. Earlier deformation analyses using a hyperbolic constitutive model for the foundation fine-grained materials did not properly represent the modulus and strength reduction and predicted extremely large permanent deformations. Cyclic triaxial laboratory tests using high-quality samples and in situ vane shear tests were used to calibrate the FLAC constitutive model herein. The resulting FLAC analysis of the unremediated dam predicted an upstream slope toe deformation of about 0.6 m, a crest settlement of about 0.6 m, and a downstream slope toe deformation of about 1.5 m using the design ground motion. Based on the estimated permanent deformations and other factors, it was decided that the anticipated upstream slope and crest deformations were tolerable and only the downstream slope had to be remediated to protect the downstream seepage control system.

Key words: earthquakes, liquefaction, numerical analysis, shear strength, post-liquefaction, slope stability.

Résumé : Dans le but d'assister la conception de la réhabilitation sismique du barrage de Tuttle Creek dans le centre est du Kansas, une analyse sismique du barrage par différence finie a été réalisée à l'aide du logiciel FLAC et des modèles constitutifs de sols UBCSAND et UBCTOT. Le logiciel FLAC est avantageux puisqu'il peut utiliser des modèles constitutifs calibrés pour un site spécifique. Des analyses antérieures faites avec un modèle constitutif hyperbolique pour des matériaux fins de fondation n'a pas pu représenter adéquatement la réduction du module et de la résistance et a prédit des déformations permanentes extrêmement grandes. Pour la présente étude, des essais triaxiaux cycliques en laboratoire avec des échantillons de qualité élevée et des essais scissométriques in situ ont été utilisés pour calibrer le modèle constitutif de FLAC. L'analyse par FLAC du barrage non réhabilité a prédit une déformation du pied de la pente en amont d'environ 0,6 m, un tassement de la crête d'environ 0,6 m, et une déformation du pied de la pente en aval d'environ 1,5 m, et ce, en utilisant les mouvements du sol de conception. Basé sur les déformations permanentes estimées et d'autres facteurs, il a été décidé que les déformations anticipées sur la pente en amont et sur la crête sont tolérables et que seulement la pente en aval doit être réhabilitée afin de protéger le système de contrôle des exfiltrations en aval.

Mots-clés : séismes, liquéfaction, analyse numérique, résistance au cisaillement, post-liquéfaction, stabilité de pente.

[Traduit par la Rédaction]

Introduction

Tuttle Creek Dam, located on the Big Blue River in the Kansas River Basin, is part of a system that provides a comprehensive plan for flood control and other functions in the Missouri River Basin. The dam was designed and constructed by the US Army Corps of Engineers (USACE), Kansas City District (KCD). Construction started in 1952 and was completed in 1960 (Lane and Fehrman 1960). Subsequent subsurface investigations and analyses conducted by the KCD led to the conclusion that seismic rehabilitation was required. Tuttle Creek Dam is located about 10 km (6 miles) north of the city of Manhattan in eastern Kansas. The embankment, primarily a rolled earthfill dam, is 2300 m (7500 ft) long and about 43 m (137 ft) high. The crest width is 15.2 m (50 ft) and the base width varies from about 430 m (1400 ft) to 490 m (1600 ft). The top of the dam is at elevation 353.3 m (1159 ft mean sea level (m.s.l.)) while the original ground surface varies, but is about 312.4 m (1025 ft m.s.l.) across the valley. The multi-purpose pool (MPP) level is at

Received 6 May 2011. Accepted 6 November 2011. Published at www.nrcresearchpress.com/cgj on 23 February 2012.

T.D. Stark. Department of Civil and Environmental Engineering, University of Illinois at Urbana-Champaign, 205 N. Mathews Ave, Urbana, IL 61801, USA.
M.H. Beaty. Beaty Engineering, LLC, Beaverton, OR, USA.
P.M. Byrne. Department of Civil Engineering, The University of British Columbia, Vancouver, BC, Canada.
G. Castro. GEI Consultants, Inc., Winchester, MA, USA.
F.C. Walberg. URS Corporation, Overland Park, KS, USA.
V.G. Perlea. US Army Corps of Engineers, Sacramento District, Sacramento, CA, USA.
P.J. Axtell. Dan Brown and Associates, Kansas City, MO, USA.
J.C. Dillon, W.B. Empson, and D.L. Mathews. US Army Corps of Engineers, Kansas City District, Kansas City, MO, USA.

Corresponding author: Timothy D. Stark (e-mail: tstark@illinois.edu).

elevation 327.9 m (1075 ft m.s.l.). The full pool, or top of the flood control pool, is at elevation 346.5 m (1136 ft m.s.l.). Thus, the dam typically operates with a freeboard of about 25.6 m (84 ft) at the MPP, which is an important consideration when evaluating the allowable earthquake-induced permanent deformations.

The foundation is characterized by a relatively thin fine-grained blanket atop a thicker zone of coarser-grained alluvial sands generally grading from fine sands beneath the blanket to coarse sands and gravels just above foundation bedrock. A typical crosssection of the dam is shown in Fig. 1*a* and Fig. 1*b* presents a plan view of the dam that shows the location of stations 30+00 to 70+00, which is the area of the seismic retrofit. Stations 10+00 to 25+00 and Stations 70+00 to 75+00 were not deemed problematic because of the presence of older terrace deposits and large upstream and downstream stabilizing berms that were installed during construction.

The main seismic source zones in east central Kansas are the Nemaha Ridge uplift zone and the Humboldt Fault zone. The maximum credible earthquake (MCE) is a magnitude 6.6 event at 20 km (12.5 miles) with a return period of about 3000 years. The MCE has a median estimate of peak horizontal ground acceleration, PHGA, of 0.28*g* and an 84th percentile estimate of 0.56*g* (Somerville et al. 2003).

Site investigations and geotechnical analyses identified the alluvial foundations sands as being susceptible to liquefaction under the MCE (USACE 1998). The clays and silts of the natural fine-grained blanket also appear susceptible to pore pressure generation and strength loss during earthquake loading (Castro et al. 2003; Boulanger and Idriss 2006). Throughout this paper the term liquefaction refers to materials that have lost significant shear stiffness due to the generation of high excess pore pressures. Liquefied materials may also suffer a substantial decrease in the available undrained strength. When the UBCSAND constitutive model is used, the foundation sands are considered to liquefy when the excess pore pressure ratio exceeds 0.7 (Marcuson and Hynes 1990; Marcuson et al. 1990).

Two lines of relief wells along the downstream toe control underseepage across the valley that is occurring through the foundation sands. A relief well collector ditch exists just downstream of the hatched line along the downsteam toe of the dam shown in Fig. 1*b*. The relief wells are parallel to both sides of the drainage ditch. Even at the MPP level, the relief wells control uplift forces near the toe and reduce the hydraulic grade line beneath the dam. If the seepage control measures were damaged or rendered inoperable by a seismic event, the dam could fail due to erosion and piping induced by the active underseepage condition.

The USACE Dam Safety Assurance Program (DSAP) provides the USACE with the means to address both seismic and hydrologic inadequacies of its nationwide system of dams. The KCD performed an extensive seismic risk management assessment for a range of remediation alternatives (USACE 2002*a*, 2002*b*). Based on the results of finite element deformation analyses, stabilizing the foundation under both upstream and downstream slopes was the preferred alternative. The models predicted unacceptably large deformations both upstream and downstream largely as a result of liquefaction and loss of strength in the foundation blanket fine-grained materials. The recommended stabilization also included an upstream cutoff wall to reduce the amount of seepage under the dam and reduce the importance of the existing seismically vulnerable pressure relief wells.

As part of this seismic remediation effort, the KCD convened an advisory panel (AP) to assist in the evaluation, analysis, design, and construction efforts for the remediation. The AP consisted of Peter M. Byrne (The University of British Columbia), Gonzalo Castro (GEI Consultants, Inc.), Robert D. Essler (RD Geotech, Ltd.), Francke C. Walberg (URS Corporation, Inc.), Peter J. Nicholson (Nicholson Consulting, LLC), and Timothy D. Stark (University of Illinois at Urbana-Champaign).

At the time the AP was mobilized the KCD had already expended considerable effort in gaining approval as described in the Seismic Evaluation Report (USACE 1999, 2002*a*, 2002*b*) and an Environmental Impact Statement (EIS) for the remediation project and re-approval would significantly delay the project. In fact, the Early Contractor Involvement construction contract with the remediation contractor was awarded about 1 month before the AP contract was awarded. Thus, AP recommendations were somewhat constrained by the Evaluation Report–EIS decision document and the remediation contract.

To facilitate the analysis and design of the seismic remediation, the KCD engaged the AP to perform a state-of-the-art seismic finite difference analysis of the unremediated dam using the Fast Lagrangian Analysis of Continua (FLAC) (Itasca Consulting Group, Inc. 2000) to better understand the zones of potential problems or permanent deformation. A key advantage of the FLAC software is that it can use site-specific calibrated constitutive models for the fine-grained blanket. Earlier deformation analyses used a hyperbolic constitutive model that could not properly represent the reduction in strength and modulus and predicted extremely large permanent deformations. Cyclic triaxial laboratory tests using high-quality samples and in situ vane shear tests were already available and could be used to calibrate the FLAC constitutive model. To accomplish this task, Michael Beaty (Beaty Engineering LLC) was retained to perform a FLAC analysis on the unremediated dam with guidance and input from the AP.

Design ground motion

Extensive work on developing the seismic hazard and ground motion parameters had been performed by USACE prior to the involvement of the AP and the FLAC analyses (USACE 1999; Somerville et al. 2003). This included deterministic and probabilistic evaluations, development of a set of four ground motions, and initial numerical analyses of the dynamic response using DYNAFLOW (Popescu 1998) and TARA-3FL (Finn and Yogendrakumar 1989) for four ground motion records. Based on SHAKE analyses performed by the KCD and preliminary finite element analyses using finite element computer programs DYNAFLOW (Popescu 1998) and TARA-3FL (Finn and Yogendrakumar 1989), the scaled Castaic record (defined in the next paragraph) was identified by the KCD to be the record giving the most damaging response in terms of crest settlement and permanent deformation at the upstream and downstream toes. The KCD considered this ground motion to yield a conservative representation of the

Fig. 1. (*a*) Typical cross section for stations 40+00 to 68+00 and (*b*) plan view showing location of stations 40+00 to 68+00 and treatment area (data from USACE 2007).

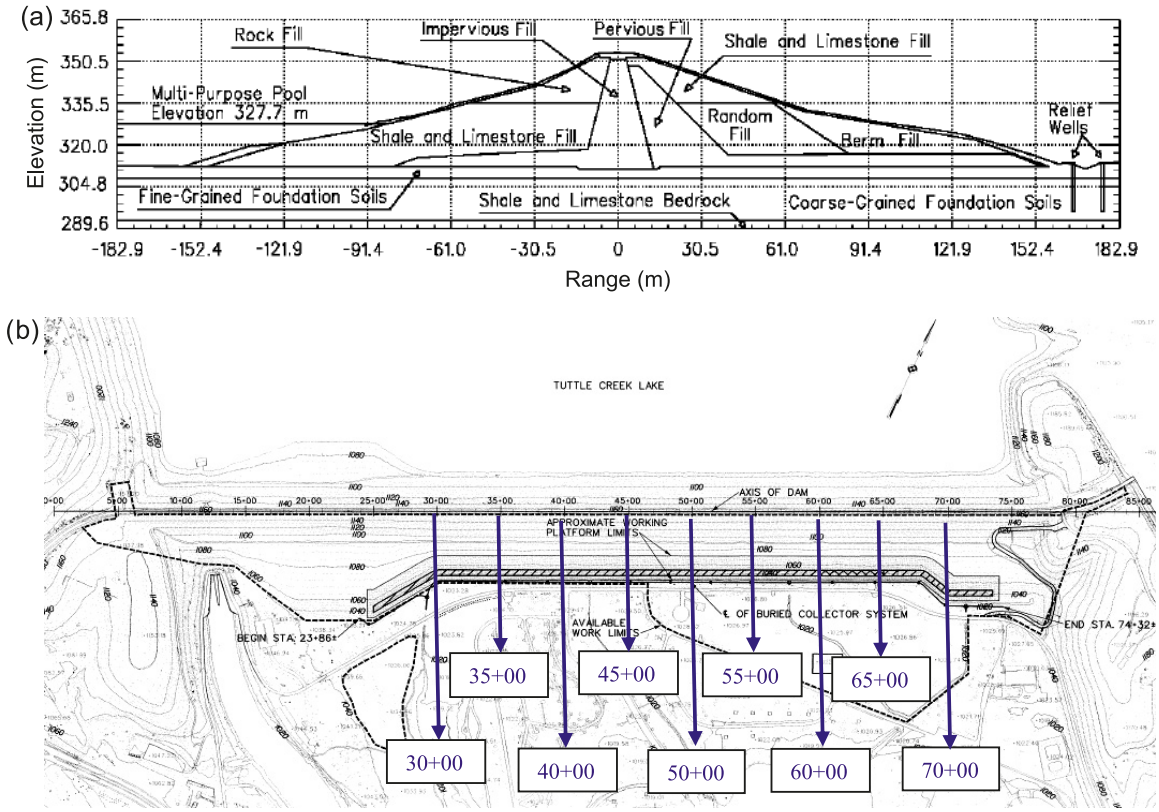

design earthquake because it matches the 84th percentile acceleration spectra for the MCE as discussed below. Because of this, the AP used the scaled Castaic record in the FLAC analyses. Of course, the AP and KCD recognize that record-to-record ground motion variability can be significant, but the design ground motion was deemed sufficiently conservative to account for these effects. Additional support for selecting the ground motion can be found in USACE (1999).

The design ground motion consists of the Castaic accelerogram from the 1971 San Fernando, California, earthquake, N69°W component, scaled to a peak acceleration of 0.3*g*. The depth and magnitude of the earthquake are 14 km (9 miles) and 6.5, respectively. The original accelerogram has a peak acceleration and duration of 0.27*g* and 40 s, respectively. The resulting time history matches the 84th percentile acceleration spectra for the MCE in a range near the fundamental period of the dam (0.3 to 0.6 s). The scaling and development of the design ground motion is discussed in Somerville et al. (2003). The design ground motion is considered conservative because the response spectra of the design event plots mostly above the evaluation mean + sigma design response spectrum for the range of natural period of the dam and yielded the most damaging response.

FLAC analysis description

Version 5.0 of the commercial computer program FLAC (Itasca Consulting Group, Inc. 2000) was used to perform the seismic deformation analysis of Tuttle Creek Dam. This program uses a two-dimensional finite difference formulation that models the embankment and foundation as a collection of plane strain elements. A two-dimensional analysis was used because of the length and consistency of the foundation and embankment geometry and materials. FLAC solves the dynamic stress-deformation problem using an explicit time stepping approach. This scheme is well suited to nonlinear evaluations and estimates of large deformations. FLAC also includes the ability to model groundwater flow using a finite difference formulation of seepage–consolidation. This capability was used to estimate the initial pore-water pressures as well as pore-water flow during earthquake shaking.

The analysis was performed using the built-in capabilities of FLAC as well as the user-defined soil constitutive models UBCSAND (Byrne et al. 2004) and UBCTOT (Beaty 2001). UBCSAND was used to model the cyclically induced pore pressures, softening, and strength loss in the foundation sands and UBCTOT was used to model the softening and strength loss in the natural fine-grained blanket. The UBCSAND input parameters were estimated from in situ penetration test data while the UBCTOT constitutive model was calibrated using laboratory cyclic triaxial compression data from high-quality samples as well as field vane shear test data on the fine-grained blanket. The embankment materials were modeled using the built-in Mohr–Coulomb stress–strain model.

Numerical model

The initial FLAC models were developed by the KCD under the supervision of Vlad Perlea (2006) and these models were adapted for use by the AP for the final evaluations. The representative cross section of the dam used for the FLAC analysis was developed by the KCD and is shown in

Fig. 1*a*. The dam and foundation were characterized by 42 distinct material zones as shown in Figs. 2*a* and 2*b*. The base of the foundation soil, i.e., bedrock, is set at a uniform elevation of 294.3 m (965 ft). The foundation surface beneath the dam is defined at elevation 312.6 m (1025 ft). The shale and limestone bedrock existing below the foundation soils is not included in the FLAC model because a rigid boundary is assumed below the foundation sands. This rigid base assumption, i.e., application of the outcrop motion at the base, is conservative compared to a more realistic compliant base. The crest of the dam is located at elevation 353.5 m (1159 ft), giving the dam a height of 40.9 m (134 ft) and a total depth of foundation soil of 18.9 m (60 ft).

The FLAC finite element mesh has 400 vertical columns and 34 horizontal layers. Twenty layers were used to model the dam while 14 layers were used for the foundation soils. Typical zone widths are about 1.5 m (5 ft) while zone heights are about 2.1 m (7 ft) in the embankment, about 1.5 m (5 ft) in the foundation sand, and about 0.9 m (3 ft) in the cohesive foundation layer.

The average element size was chosen to facilitate the transmission of the high-frequency (short wavelength) shear waves induced by the design ground motion. The primary response frequency of the embankment-foundation system prior to the generation of high pore pressures was estimated to be about 1.8 Hz. Ideally, frequencies greater than at least 2 to 3 times this primary frequency should be transmitted through the model without a significant loss in accuracy. A common guideline for ensuring adequate transmission is to have at least 10 elements defining one wavelength at the transmission frequency of interest. Assuming shear stiffness similar to the maximum shear modulus (G_{max}), the adopted mesh can transmit frequencies in excess of about 10 Hz (16 Hz in the foundation sand, 21 Hz in the fine-grained layer, and 10 Hz in the embankment). A modulus reduction factor of 0.5 allows frequencies in excess of 5 Hz to be transmitted accurately. These estimates reflect conditions at the downstream shell and within the foundation materials beneath the outer downstream shell.

The same mechanical boundary conditions were used for both static and dynamic loading: the bottom of the model was fixed in both the vertical and horizontal directions, while the left and right edges of the model were fixed in the horizontal direction. The horizontal earthquake motion was then applied to each of these boundaries for the dynamic analysis. Thus, the bottom and sides of the model form a rigid box whose movement is defined by the input ground motion. A rigid rather than a compliant boundary was used for the dynamic loading because of the significant impedance contrast between the bedrock and foundation sand. The use of fixed vertical boundaries was adopted in the original FLAC model developed by the KCD. This simple boundary is not ideal, but was considered acceptable for the later analyses because of the large distance between the boundaries and the dam footprint: 132.7 m (435 ft) on the upstream side and 128.1 m (420 ft) on the downstream side.

Material zones and properties

The embankment of Tuttle Creek Dam is relatively complex with many different subzones as shown in Fig. 2. A general description of the various embankment zones and numbering system is provided in Table 1.

The foundation materials can be characterized by two distinct material types: a continuous fine-grained blanket directly beneath the dam (thin layer under entire embankment numbered CL-1 to CL-5 in Fig. 2) and the underlying foundation sands (FS-1 to FS-28 in Fig. 2). Each of the foundation sand layers was divided into subzones that were used to represent the differences in density or blowcount that are due to geologic–depositional and confining pressure differences. Table 2 gives a general description of the various materials in the foundation soil.

Geophysical tests were available for many of the embankment and foundation zones. The tests were conducted at the crest, downstream slope, and downstream toe of the dam. These results are not included because of space constraints. Additional descriptions of the foundation sands and fine-grained blanket is provided below.

Foundation sand

The modeling and evaluation of the foundation sands was primarily on blowcounts from standard penetration tests (SPTs). These blowcounts were normalized to $(N_1)_{60}$ (which is the blow count corrected for the effective stress and energy level used in the SPT) values by the KCD. The KCD also corrected the $(N_1)_{60}$ values for the amount of fines content present in the zone using the fines content correction proposed by Youd et al. (2001). The SPT results for the foundation sands are summarized in Table 3 and these data were derived from Perlea (2006). The 33rd-percentile $(N_1)_{60}$ value was chosen as representative of the sand within any subzone. The 33rd-percentile $(N_1)_{60}$ is the value of $(N_1)_{60}$ within a subzone where two-thirds of the recorded $(N_1)_{60}$ values are larger and one-third are smaller. Use of the 33rd-percentile $(N_1)_{60}$ was typical practice for USACE projects and is suggested in the USACE older version of the slope stability manual (USACE 1970).

Fine-grained blanket

The KCD had previously obtained high-quality samples of the fine-grained blanket and had conducted a series of laboratory triaxial compression and in situ tests to better estimate the stress–strain behavior for deformation analyses (Castro et al. 2003). Fifteen cyclic triaxial compression tests were performed by GEI Consultants, Inc. at stresses corresponding to locations beneath the crest, downstream mid-slope, and downstream toe. The triaxial tests revealed two key aspects of the fine-grained blanket behavior: (*i*) pore pressures are generated by cyclic loading, which produce a significant decrease in soil stiffness, and (*ii*) undrained shear strength, S_u, of the fine-grained blanket decreases as the cyclically induced shear strain increases (Castro 1999; GEI Consultants, Inc. 2000). Two tests were also performed in triaxial extension to evaluate the potential for anisotropy in the undrained strength. Although not conclusive, these tests suggest the peak undrained strength of this clay is relatively isotropic.

Vane shear testing was used to verify the peak undrained strength ratio obtained from triaxial compression testing of the fine-grained blanket and to establish the strength loss relationship for shear strains greater than 15%. The vane shear test equipment was a Roctest M-1000 device. A 75 mm (approximately 3 inch) vane diameter was used at the downstream toe and a 50 mm (approximately 2 inch) diameter vane was used under the dam slopes because of the higher shear resistance.

Fig. 2. Material zoning for (*a*) upstream and (*b*) downstream of Tuttle Creek Dam.

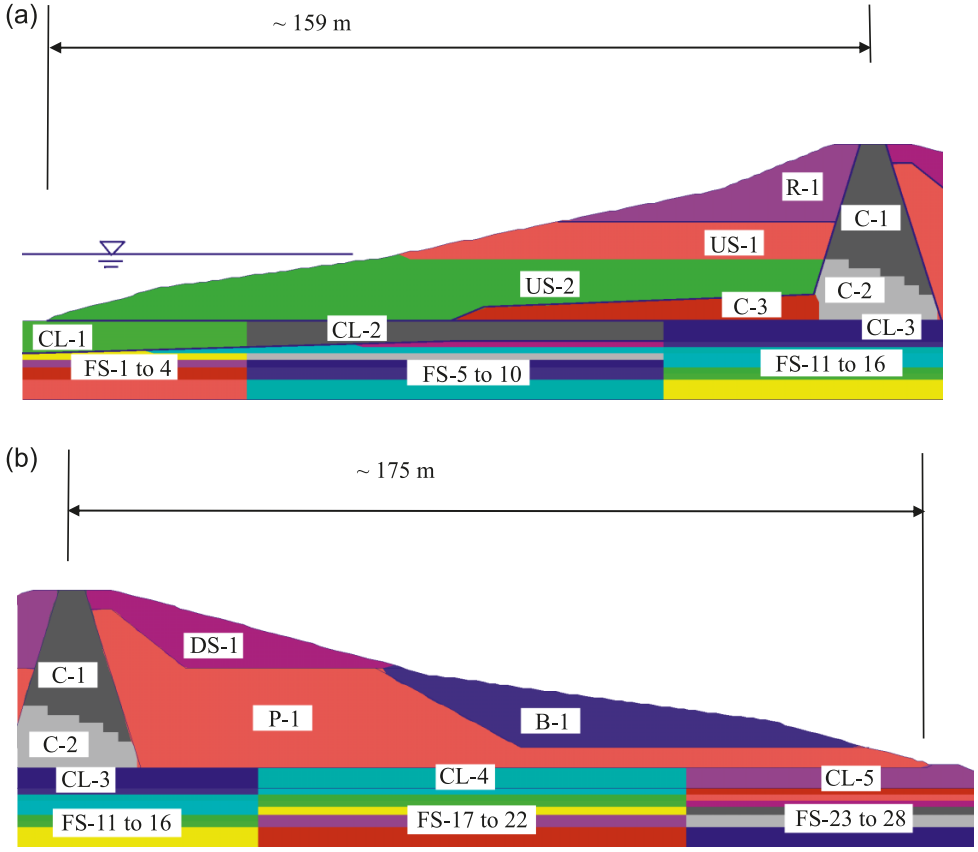

Table 1. Embankment fill materials.

Material	General description	Symbol	Approx. elevation range (m/ft m.s.l.)
Impervious core	Low-plasticity lean clay, LL = 30 to 35, PI = 10 to 15.	C-1	353.5–327.9 / 1159–1075
		C-2	327.9–312.6 / 1075–1025
		C-3	318.7–312.6 / 1045–1025[a]
Rockfill	Upper 1.5 m is durable limestone and approximately 10% hard shale. The rest contains maximum 33% shale.	R-1	353.5–335.5 / 1159–1100
Shale and limestone	Dense, relatively impermeable material with about 30% passing No. 200 sieve and occasional lenses of cleaner, highly pervious limestone fill.	US-1	335.5–327.9 / 1100–1075
		US-2	327.9–312.6 / 1075–1025
		DS-1	353.5–335.5 / 1159–1100
Berm	Mostly lean clay with layers of silty, sandy, and gravelly materials and light compaction.	B-1	335.5–317.2 / 1100–1040
Pervious fill	Free-draining sand or sand and gravel.	P-1	349.2–312.6 / 1145–1025

Note: LL, liquid limit; PI, plastic index.

[a]Upstream impervious fill.

The undisturbed laboratory and vane shear test results were used to develop the relationship between shear strain induced by cyclic loading and the undrained shear strength ratio as shown in Fig. 3. The undrained strength ratio is defined as the undrained shear strength (S_u) expected to occur in simple shear loading divided by the vertical effective consolidation stress (sigvc′) as shown in Fig. 3. The use of a peak undrained strength ratio of 0.35 was verified for the natural fine-grained blanket even though this strength ratio is at the upper range for a normally consolidated clay in simple shear. The verification included the performance of vane tests at various rates of rotation, which led to the conclusion that the somewhat elevated undrained strength ratio was not the result of significant drainage during the vane shear test. The undrained strength ratio of 0.35 may be somewhat elevated because the fine-grained blanket is overconsolidated due to seepage forces and the shear stresses imposed by the embankment slopes, the silty nature of the material versus a homogenous soft clay, uncertainties in the applied vertical effective stress, and possible desiccation prior to embank-

Table 2. Foundation soil materials.

General description[a]	Location	Material symbol	Approx. elevation range (m/ft m.s.l.)
Natural fine-grained blanket:			
Low-plasticity clays (CL), silty clays (CL-ML), clayey silts (ML-CL), and some silts (ML). Generally less than 20% fine sand. Moisture content, w = 23%–44%, LL = 21–44, PI = 4–27. Void ratio, e = 0.6–1.0 (av. 0.8) at dam toe, 0.5–0.9 (av. 0.73) under mid-slope, 0.66 under crest.	U/S toe	CL-1	312.6–305.0 / 1025–1000
	U/S slope	CL-2	312.6–308.1 / 1025–1010
	Axis	CL-3	312.6–308.1 / 1025–1010
	D/S slope	CL-4	312.6–308.1 / 1025–1010
	D/S toe	CL-5	314.2–308.1 / 1030–1010
Upper sand:			
Sand (SW, SP), silty sand (SM), sand with silt (SP-SM), sand with clay (SP-SC), silt (ML), clayey sand (SC). Some lean clay (CL) layers.	U/S toe	FS-1 / 3	305.0–298.9 / 1000–980
	U/S slope	FS-5 / 9	308.1–298.9 / 1010–980
	Axis	FS-11 / 15	308.1–298.9 / 1010–980
	D/S slope	FS-17 / 21	308.1–298.9 / 1010–980
	D/S toe	FS-23 / 27	308.1–298.9 / 1010–980
Lower sand:			
Same as above, plus occasional gravel grading to coarse sand and gravel just above the foundation rock.	—	FS-4	298.9–294.3 / 980–965
		FS-10	298.9–294.3 / 980–965
		FS-16	298.9–294.3 / 980–965
		FS-22	298.9–294.3 / 980–965
		FS-28	298.9–294.3 / 980–965

Note: D/S, downstream; U/S, upstream.

[a]Classified according to ASTM (2006).

ment construction. Review of the vane shear data also confirmed the residual strength ratio of 0.12 shown in Fig. 3, which was measured after several vane rotations. A friction angle of 30° and a cohesion intercept of zero were adopted for the drained strength parameters of the fine-grained blanket.

Constitutive models and properties

The constitutive models used for the Tuttle Creek Dam analysis were selected for each material zone based on anticipated material behavior. An effective stress model with full coupling between the mechanical and groundwater flow processes was used for the foundation sands to address the effects of shear-induced pore pressures caused by the earthquake shaking of saturated sands. A total stress model that captures the softening and strength loss with accumulating strain during cyclic loading was used for the fine-grained blanket. A simpler linear elastic–plastic stress–strain model that uses average secant stiffness and an appropriate strength–failure envelope was selected for the embankment materials because the strength loss due to cyclic loading was expected to be small owing to the materials involved and level of densification during construction. The following sections provide additional details on the selected constitutive models.

UBCSAND: foundation sands

The foundation sands were modeled using the UBCSAND constitutive model. This model considers the effects of shear-induced pore pressures during earthquake shaking, which can result in significant changes in effective stress. The UBCSAND model generates pore pressures in saturated elements in a manner consistent with observations from laboratory tests whether or not the sand is in a contractive or dilative state. The model follows an elastic–plastic formulation where the hardening and flow rule relationships are based on changes in stress ratio, η, where η is defined as the maximum shear stress, τ, divided by the mean effective stress, σ'_m, on the principal planes. A hyperbolic relationship is used to relate increases in stress ratio to increments of plastic shear strain, γ_p. The relationship between increments of plastic shear strain, γ_p, and plastic volumetric strain, ε_{vp}, is defined by a function of the current stress ratio and the constant volume friction angle, ϕ_{cv}. Strain increments occurring at η less than $\sin\phi_{cv}$ are contractive, while those occurring at $\eta > \sin\phi_{cv}$ are dilative. The stress–strain response for loading after the generation of high pore pressures tends to be governed by dilation, which results in the classic concave or banana-shaped stress–strain loops observed in laboratory cyclic triaxial compression tests. Additional details on the constitutive model are provided in Byrne et al. (2003, 2004).

Prior research and case histories show that FLAC analyses using a calibrated UBCSAND model can provide useful predictions of the seismic response and permanent displacements of a dam subjected to a design ground motion. Some of the case histories that have been successfully analyzed using FLAC are Lower San Fernando Dam by Naesgaard et al. (2006), Mochi Koshi Tailings Dams described by Marcuson et al. (1979) and analyzed by Byrne and Seid-Karbasi (2003), and centrifuge tests (Byrne et al. 2003, 2004; Yang et al. 2004; Naesgaard et al. 2005; Seid-Karbasi et al. 2005).

Table 3. $(N_1)_{60}$ values in foundation for stations 35+00 to 70+00.

Location	Material symbol	Approx. elevation range (m/ft m.s.l.)	No. of available $(N_1)_{60}$ values	$(N_1)_{60}$ 33rd percentile	Clean sand $(N_1)_{60,cs}$ 33rd percentile
Fine-grained layer:					
U/S toe	CL-1	312.6–305 / 1025–1000	33	4.5	N/A
U/S slope	CL-2	312.6–308.1 / 1025–1010	69	13.5	N/A
Axis	CL-3	312.6–308.1 / 1025–1010	43	11.5	N/A
D/S slope	CL-4	312.6–308.1 / 1025–1010	41	10.8	N/A
D/S toe	CL-5	314.2–308.1 / 1025–1010	56	3.2	N/A
Upper sand:					
U/S toe	FS-1	305–303.5 / 1000–995	14	12.7	14.1
	FS-2	303.5–302 / 995–990	9	22.9	26.3
	FS-3	302–298.9 / 990–980	17	22.9	26.3
U/S slope	FS-5	308.1–306.5 / 1010–1005	29	27.2	34.0
	FS-6	306.5–305 / 1005–1000	35	21.0	26.7
	FS-7	305–303.5 / 1000–995	30	17.7	21.1
	FS-8	303.5–302 / 995–990	27	19.3	23.4
	FS-9	302–298.9 / 990–980	63	28.7	30.5
Axis	FS-11	308.1–306.5 / 1010–1005	16	20.6	25.4
	FS-12	306.5–305 / 1005–1000	15	22.6	27.7
	FS-13	305–302 / 1000–990	32	12.4	17.7
	FS-14	302–300.4 / 990–985	19	20.0	25.2
	FS-15	300.4–298.9 / 985–980	26	23.0	28.2
D/S slope	FS-17	308.1–306.5 / 1010–1005	26	26.0	30.0
	FS-18	306.5–305 / 1005–1000	28	24.0	27.7
	FS-19	305–303.5 / 1000–995	27	17.6	20.3
	FS-20	303.5–302 / 995–990	28	20.5	23.1
	FS-21	302–298.9 / 990–980	49	24.4	26.9
D/S toe	FS-23	308.1–306.5 / 1010–1005	13	11.0	13.7
	FS-24	306.5–305 / 1005–1000	40	11.7	13.4
	FS-25	305–303.5 / 1000–995	29	15.5	18.4
	FS-26	303.5–302 / 995–990	26	18.0	21.5
	FS-27	302–298.9 / 990–980	65	21.4	25.6
Lower sand:					
U/S toe	FS-4	298.9–294.3 / 980–965	8	34.5	36.9
U/S slope	FS-10	298.9–294.3 / 980–965	64	26.0	28.0
Axis	FS-16	298.9–294.3 / 980–965	36	23.6	28.9
D/S slope	FS-22	298.9–294.3 / 980–965	35	24.4	26.9
D/S toe	FS-28	298.9–294.3 / 980–965	43	21.1	23.8

Note: N/A, not applicable.

Fig. 3. Undrained strength loss with increasing seismically induced shear strain for the fine-grained blanket. S_{u_peak}, peak undrained shear strength; S_{u_ss}, undrained shear strength at maximum shear strain.

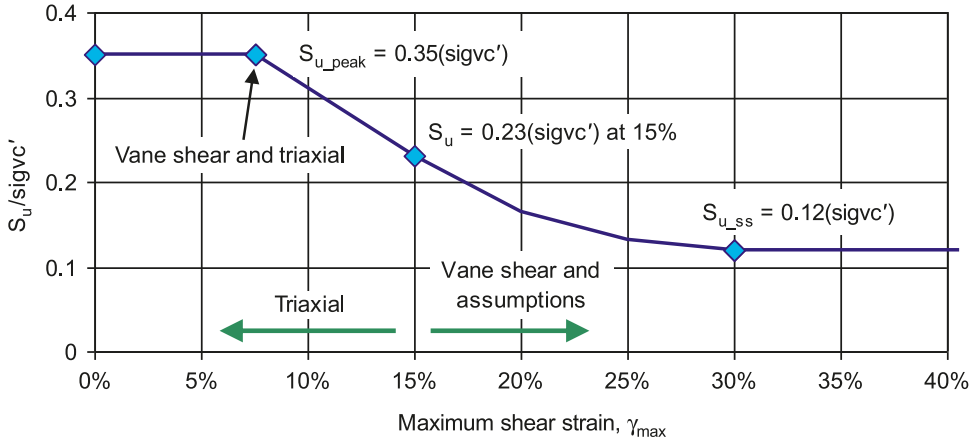

The basic parameters required for the UBCSAND model are the elastic and plastic shear modulus numbers, the elastic bulk modulus number, stress exponents that relate the shear and bulk moduli to changes in mean effective stress, the constant volume friction angle, ϕ_{cv}, the friction angle at failure, ϕ_f, and the failure ratio for the hyperbolic relationship, R_f. Generic parameters have been developed for UBCSAND to approximate typical sand behavior with a particular emphasis on liquefaction triggering as captured in the semi-empirical liquefaction triggering chart from Youd et al. (2001). These generic parameters consider such factors as typical relationships between shear-wave velocity, V_s, and penetration resistance; semi-empirical charts relating cyclic stress ratio to the onset of liquefaction; and trends in stress–strain behavior observed in laboratory triaxial element tests.

Because no laboratory stress–strain data were available for the foundation sands below Tuttle Creek Dam, the input parameters for the UBCSAND model were based primarily on the generic input parameters. These parameters provide a reasonable engineering estimate of the stiffness, the generation of pore pressures due to cyclic loading, and the post-liquefaction stress–strain behavior. The selected parameters were estimated from available $(N_1)_{60}$ blowcounts, V_s measurements, and soil classification data. Some adjustments to the parameters were made to consider the strength values provided by the KCD (ϕ_{cv} was reduced from 33° to 30°) and to incorporate the confining stress effect (K_σ) for the range of stresses that exist beneath Tuttle Creek Dam. The K_σ relationship used for Tuttle Creek Dam was provided by the KCD and is given in Youd et al. (2001) with an exponent coefficient "*f*" equal to 0.7.

UBCSAND models the behavior of liquefied sand including the soft loading response typical of dilative response and the softening effects of pore-water inflow. The predicted response of liquefied zones tends to demonstrate soft and weak behavior with shear stresses being distributed to the stiffer, nonliquefied zones. The strength mobilized in the liquefied UBCSAND elements is a function of many factors including parameters related to relative density, the imposed strains, the permeability magnitude and distribution, and the mesh size. However, the actual behavior of liquefied sand under field conditions may be extremely complex and include mechanisms that are not directly, or only partially, considered in the UBCSAND model. These mechanisms may include void redistribution and mixing of soil layers at high shear strains. In addition, the strength mobilized by UBCSAND through dilation was not capped at an assumed value of critical state strength.

Because the strengths mobilized by UBCSAND after liquefaction can exceed estimates of post-liquefaction strength derived from case histories, the application of UBCSAND to Tuttle Creek Dam considers the potential for a post-earthquake loss in strength. This post-liquefaction or liquefied strength was estimated using published results from back-analysis of case histories (Seed and Harder 1990; Stark and Mesri 1992; Olson and Stark 2002) using 33rd-percentile values for blowcount, which is typical for USACE projects (USACE 1970) as discussed previously. The sands in the foundation of Tuttle Creek Dam are generally substantially denser than for the case histories, which were conservatively applied to Tuttle Creek Dam. Due to the presence of the continuous fine-grained layer overlying the alluvial foundation sands, the potential for void ratio redistribution and pore-water accumulation or buildup beneath this layer was a key concern for post-liquefaction stability of the dam. The use of liquefied strengths conservatively developed from flow failure case histories is intended to represent the effects of the unfavorable conditions and mechanisms. These strengths are generally lower than would be expected from undrained behavior of liquefied sand as observed in laboratory triaxial testing (Kokusho 1999; Kokusho and Kojima 2002).

The liquefied strengths were assigned after the end of strong shaking because it was considered likely that it would take some time for the full strength degradation to occur. While loose sands might quickly degrade to the minimum strength, the somewhat denser sands at Tuttle Creek Dam would likely require time for the full strength loss to occur due to void redistribution from pore-water migration. This assumption is supported by many case histories where post-liquefaction failure has been delayed until sometime after the end of the earthquake (Seed et al. 1975). It is also consistent with post-earthquake stability analysis that has traditionally been performed using limit equilibrium techniques.

The post-earthquake analysis assigned liquefied strengths to any UBCSAND element that had experienced a maximum pore pressure ratio, r_u, of 0.7 or higher during the earthquake. For each of these elements, a simple Mohr–Coulomb constitutive model is substituted for the UBCSAND model at the completion of the earthquake analysis. A softened shear modulus and an undrained strength equal to the selected liquefied strength for that element are assigned. The $r_u \geq 0.7$ limit was selected as a reasonable criterion for identifying zones that should be considered susceptible to strength loss. Although liquefaction is sometimes defined as soil achieving an excess pore pressure ratio of 1.0, it often requires little additional loading for pore pressures to increase from $r_u = 0.7$ to 1.0. This is demonstrated by the relationship between r_u versus the factor of safety against liquefaction presented by Marcuson and Hynes (1990), Marcuson et al. (1990), and Seed and Harder (1990). The range of factor of safety at an r_u value of 0.7 is 1.0 to 1.07 for sands. In addition, liquefied soils under a significant static shear stress may never achieve an r_u of 1.0.

The calibration of UBCSAND was performed by analyzing single elements in a cyclic simple shear mode. Up to three element calibrations were performed for each of the foundation sand zones. The model parameters were adjusted until the element liquefied in 15 cycles of loading, which is the number of uniform loading cycles that is considered to be consistent with the Youd et al. (2001) and Idriss and Boulanger (2008) triggering chart. After obtaining agreement between the FLAC elements and the Youd et al. (2001) triggering chart multiplied by the K_σ factor, the UBCSAND model was considered calibrated for application to the foundation sands at Tuttle Creek.

The UBCSAND model was also calibrated by comparing values of maximum shear modulus, G_{max}, estimated from field shear-wave velocity tests to values of G_{max} estimated from the calibrated UBCSAND model. If there was good agreement between the measured and calculated values of G_{max}, the calibrated input parameters were considered to be

verified to the extent possible against the limited available information. These V_s values in the foundation sand ranged from 186 to 393.5 m/s (610 to 1290 ft/s). The corresponding values of V_s predicted by the calibrated UBCSAND elements are in reasonable agreement, i.e., the V_s values differ on average by about 15%. A difference of 15% in V_s in a portion of the model was not considered significant because it equates to a difference of less than 15% in the fundamental period of the structure.

UBCTOT: fine-grained blanket

The stress–strain response for elements representing the fine-grained blanket underlying the dam was modeled using a total stress approach. UBCTOT is a hysteretic stress–strain model used for the fine-grained blanket, and is an extension of the original UBCTOT constitutive model developed for liquefiable sands by Beaty (2001). Key aspects of the material behavior that are captured by the extended UBCTOT model include nonlinear stress–strain loops prior to liquefaction, the reduction in stiffness with generation of cyclically induced pore pressures, the change from convex to concave stress–strain loops at liquefaction, and the decrease in undrained strength with increasing seismic shear strain.

The UBCTOT constitutive model assumes the fine-grained soil can exist in one of two states during the earthquake: preliquefaction (or nonliquefied) and post-liquefaction. The preliquefaction behavior is represented with a hysteretic model that is based on an assumed hyperbolic relationship between shear stress and shear strain. The post-liquefaction response is modeled using a bi-linear representation of the concave stress–strain relationship during loading. The loading curve is determined by the following two linear moduli: an initially soft modulus (G_{slack}) immediately after a change in shear stress direction, and a somewhat stiffer modulus at higher stress levels (G_{liq}). The loading modulus switches from G_{slack} to G_{liq} at the instant the previous maximum (or minimum) value of shear strain is exceeded. These two moduli approximate a concave upward loading shape after liquefaction (see Fig. 4). A third, stiffer modulus is used for unloading as shown in Fig. 4. Soft loading moduli and a stiff unloading modulus allow for the accumulation of strain through ratcheting behavior. The formulation of this model is described in detail in Beaty (2001) and the ratcheting or increasing of shear strain continues until seismic loading ceases.

The UBCTOT model behavior was calibrated using laboratory cyclic triaxial compression test results on high-quality samples of the fine-grained blanket (Castro 1999, 2000*a*, 2000*b*; Castro et al. 2003). The calibration involves simulating a cyclic triaxial compression test with FLAC and adjusting the input parameters so the FLAC model yields a similar stress–strain response as measured in the laboratory. Once the FLAC stress–strain response was calibrated to the set of triaxial specimen results, the model could be applied to all of the elements representing the fine-grained blanket in the mesh. Because the UBCTOT model is formulated for plane strain conditions, the triaxial tests were simulated by assuming plane strain compression in FLAC. The plane strain compression produces a stiffer soil response than triaxial compression, therefore the shear parameters from the calibrated FLAC element are expected to give a somewhat soft representation (lower modulus) of the fine-grained soil.

Fifteen cyclic triaxial tests were performed by GEI Consultants, Inc. (2000) at stresses corresponding to locations beneath the crest, downstream mid-slope, and downstream toe. The tests that liquefied in less than about 20 cycles are more indicative of the soils that will liquefy during the design ground motion. A total of 10 tests satisfied this criterion and were used for the calibration of the FLAC hysteretic model.

The laboratory triaxial compression tests show that the undrained strength, S_u, of the fine-grained blanket decreases as the cyclically induced shear strain increases (GEI Consultants, Inc. 2000). To address this potential softening, the UBCTOT model evaluates S_u as a function of the maximum shear strain, γ_{max}, that has been experienced by the element due to the earthquake loading. The value of γ_{max} may occur in any direction and reflects the actual shear strain state of the element rather than a summation of γ_{max} increments. The calculated value of γ_{max} represents the average strain over each element that is typically about 0.9 m high.

The potential reduction in undrained strength related to shear strain is continuously evaluated in each element of the fine-grained blanket whether or not the element has liquefied. Figure 3 shows the relationship between undrained strength ratio, S_u/sigvc′, and γ_{max} adopted for the analysis of the unremediated dam. The shape of the relationship for values of γ_{max} between 0% and 15% was developed by Castro (2000*a*) based on the laboratory cyclic triaxial test results on high-quality samples of the fine-grained blanket. The relationship at shear strains greater than 30% is based on field vane shear tests at large displacements conducted by the KCD. The relationship for shear strains between 15% and 30% was estimated to provide a smooth transition between the triaxial compression test results and the minimum undrained strength obtained from the field vane shear tests.

Embankment materials

The various zones of the embankment have been characterized by the KCD as material that will not experience either a significant increase in pore pressure or loss of strength during the design ground motion. Thus, the critical embankment aspects to be modeled are the shear and bulk stiffness–modulus, shear strength, and damping. The simple Mohr–Coulomb plasticity model is used to model this element behavior.

The Mohr–Coulomb model assumes linear elastic behavior for all stress states below the failure envelope. This envelope is defined by a friction angle and cohesion intercept, and element failure is identified by comparing the Mohr's circle for stress to the failure envelope. In this context, element failure means only that plastic strains occur. When the total strain increment over any time step attempts to increase the stress state above the failure envelope, the plasticity formulation corrects this stress state back to the failure envelope by computing the portion of the total strain increment that consists of plastic irrecoverable strains. The materials modeled with the Mohr–Coulomb constitutive model are assumed to have a dilation angle of zero, which means that plastic shear strains are computed during element failure without any corresponding plastic volumetric strain.

The key input parameters for the Mohr–Coulomb model are unit weight, elastic shear modulus, elastic bulk modulus, friction angle (ϕ), cohesion intercept (c), and damping. The unit weight and strength parameters for the embankment

Fig. 4. Stress–strain behavior for post-liquefaction with static shear bias in the fine-grained blanket captured by the UBCTOT model.

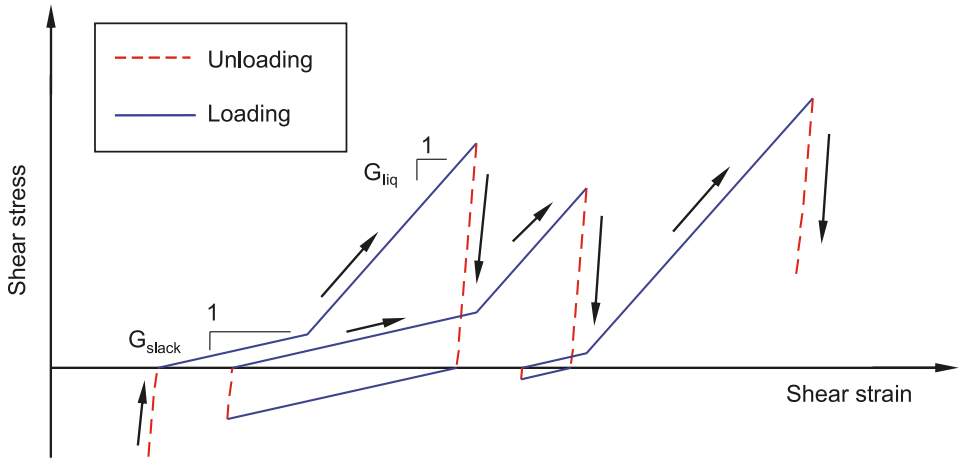

zones were developed by the KCD and are shown in Table 4. The elastic stiffness properties were estimated from the V_s measurements shown in Table 5. The V_s values were first converted into equivalent G_{max} values, which were then applied to each element using the stress-level dependence described by eq. [1].

$$[1] \qquad G_{max} = G_{max1}\left(\frac{\sigma'_y + \sigma'_x}{2}\right)^{0.5}$$

where $G_{max1} = \rho V_{s1}^2$, ρ is the density, V_{s1} is the shear-wave velocity, and σ'_y and σ'_x are the vertical and horizontal effective stresses, respectively.

The elastic bulk modulus is assumed to equal G_{max} for drained conditions. This corresponds to an initial, low-strain Poisson's ratio of 0.125 for unsaturated or drained conditions. For saturated zones, an elastic bulk modulus for the water equal to 5.07×10^5 kPa (1.06×10^7 psf) was also assigned. The elastic shear modulus is reduced from G_{max} to account for a reduction in the secant shear modulus with cyclic strain. The appropriate amount of reduction was estimated from a series of equivalent linear analyses using the computer program SHAKE (Idriss and Sun 1992). Modulus reduction values between 0.5 and 1.0, depending upon the material zone and location, were used for Tuttle Creek Dam.

The strength parameters c and ϕ are used directly for all unsaturated zones. An equivalent undrained strength, S_u, is assigned in all saturated zones. This value of S_u is estimated from the undrained strength parameters and the mean effective stress of the element at the start of the design ground motion.

FLAC analysis procedure

The numerical analysis procedure consisted of three distinct phases: (*i*) estimating the initial stress state of the model by establishing the geometry and pre-reservoir stresses (dam construction analysis) and then performing a reservoir-seepage analysis, (*ii*) determining the response of the model to the input ground motion, and (*iii*) evaluating the potential effect of liquefied strength in the liquefied sand elements after the end of the earthquake shaking.

Initial state of stress

The building of the dam geometry in the numerical model is an approximate simulation of the actual construction of the dam. The primary goal of this analysis is to establish a reasonable stress state for use as an initial condition for the dynamic analysis. Detailed modeling of the construction and reservoir operation stages was not considered necessary due to the many sources of uncertainty in estimating the initial stress state. For example, drained strengths were used for the cohesive layer rather than a complex representation of the potential undrained response. The simple Mohr–Coulomb model with stress-dependent stiffness properties was also considered appropriate.

The first step is to determine the initial stresses in the foundation without the dam. A hydrostatic groundwater condition was assumed with the phreatic surface at elevation 309.9 m (1016 ft m.s.l.) or 2.7 m (9 ft) below ground surface. Once the foundation is in equilibrium under gravity loading, a single row of dam elements is added to the model. The model is again brought to equilibrium and the process of adding layers is repeated until the entire dam is constructed. The rows of elements in the Tuttle Creek Dam model are roughly 2 m (6 ft) high, or about 1/20th of the dam height. The Mohr–Coulomb model was used to represent the nonlinear stress–strain behavior of the soil by assuming an equivalent linear elastic modulus and drained strength parameters. This linear shear modulus is a fraction of the estimated G_{max} of the element. Stress-dependent values of shear and bulk stiffness were used by modifying the moduli with changes in stress. The moduli were assumed to be a function of the square root of the mean effective stress.

The effects of the reservoir on the pore-water conditions were evaluated by performing a transient seepage analysis that reaches a steady-state seepage condition. The reservoir surface elevation was assumed to be elevation 327.9 m (1075 ft m.s.l.), which corresponds to the operating pool level. Pore pressures equivalent to hydrostatic reservoir conditions were applied to the surface of the model submerged by the reservoir. An equivalent mechanical pressure was also applied to this surface to simulate the reservoir. The boundary conditions on the downstream edge of the model were

Table 4. Embankment properties for Mohr–Coulomb model.

	Unit weight (kN/m^3)			Drained strength		Undrained strength	
Material	Dry	Moist	Saturated	c' (kPa)	ϕ' (°)	c (kPa)	ϕ (°)
Impervious fill[a]	15.7	18.9	18.9	0	30	Peak: 38.3	11.3
						Residual: 14.9	5.7
Shale and limestone fill[b]	17.3	20.4	21.2	0	28	9.6	19.8
Berm	14.5	17.3	—	0	28	—	—
Pervious fill[c]	17.0	19.6	20.4	0	38	0	38
Rockfill	18.9	18.9	—	0	40	—	—

Note: 1 kN/m^3 = 6.36 pounds per cubic foot (pcf); 1 kPa = 20.9 pounds per square foot (psf). Prime symbol indicates values relate to drained strength.

[a]Undrained strength of impervious fill assumed equal to drained strength in FLAC analyses.

[b]If shale and limestone fill is saturated, $\phi = 0$ and c = undrained strength of 9.6 kPa.

[c]Undrained strength of pervious zone cannot be greater than initial drained strength.

Table 5. Shear-wave velocities in the embankment, foundation, and bedrock.

Material	Symbol	Approx. range of elevations (m/ft m.s.l.)	Shear-wave velocity (ft/s)
Embankment:			
Impervious core	C-1	353.3–327.7 / 1159–1075	1100
	C-2	327.7–312.4 / 1075–1025	1490
Berm	B-1	335.3–317 / 1100–1040	960
Pervious fill	P-1	349–312.4 / 1145–1025	1150
Foundation:			
Cohesive layer			
Axis	CL-3	312.4–307.8 / 1025–1010	1090
D/S slope	CL-4	312.4–307.8 / 1025–1010	960
D/S toe	CL-5	313.9–307.8 / 1030–1010	610
Upper sand			
Axis	FS-11…15	307.8–298.7 / 1010–980	1090
D/S slope	FS-17…21	307.8–298.7 / 1010–980	960
D/S toe	FS-23…27	307.8–298.7 / 1010–980	610
Lower sand			
Axis	FS-16	298.7–294.1 / 980–965	1290
D/S slope	FS-22	298.7–294.1 / 980–965	1120
D/S toe	FS-28	298.7–294.1 / 980–965	870
Upper 6 m of bedrock			
Free field	—	294.1–288 / 965–945	3100
Below shells	—	294.1–288 / 965–945	3230
Below crest	—	294.1–288 / 965–945	3530
Bedrock deeper than 6 m	—	Below 228 / 945	4000 (assumed)

Note: 1 ft = 0.3048 m.

assumed to equal a hydrostatic stress state with the phreatic surface at elevation 310.8 m (1019 ft m.s.l.) or 1.8 m (6 ft) below the ground surface. The pore-water conditions at the upstream vertical boundary of the model were adjusted until the pressure distribution predicted in the analysis beneath the upstream shell was slightly higher than the available piezometer measurements.

The seepage analysis was performed using a coupled mechanical-groundwater flow process. This enabled the mechanical effects caused by changes in effective and shear stress to be properly included. The relief wells were not modeled in this analysis. The wells control the level of the phreatic surface near the downstream toe, increase downstream toe stability and erosion protection, and reduce liquefaction potential in the toe area. Thus, it is conservative to not include the relief wells in the deformation analysis. The relief wells also would impact the seepage condition near the downstream toe and beyond of the dam, but have little effect under the dam. The wells are also not modeled in the dynamic phase or the post-dynamic phase of the analysis, to provide a worst-case scenario of permanent deformation for evaluating the operability of the wells after the design ground motion.

Dynamic response

Several modifications were made to the model to convert it from the static analysis to the dynamic analysis, which included

- The constitutive model in the foundation sand was changed from Mohr–Coulomb to UBCSAND.
- The constitutive model in the fine-grained blanket was changed from Mohr–Coulomb to the hyperbolic UBCTOT strain-softening model.

- Viscous damping of 2% to 4% of critical was applied to the embankment elements using a Raleigh formulation with a center frequency of 1.5 Hz. A lower-bound estimate of damping was used to address the impact of static shear stress on the anticipated stress–strain loops and to account for the hysteretic damping that would be modeled at times of shear yield. Only 1% of critical damping was assigned to the foundation elements using the Rayleigh formulation because the constitutive models in these materials include hysteretic damping.
- The design ground motion was applied to the boundary.
- An algorithm was defined that computes the excess pore pressure ratio in the foundation sand and stores the maximum value of r_u experienced by each element to determine whether or not an element liquefies.

The model was then analyzed for 40 s of the design earthquake record.

Post-liquefaction behavior

The post-dynamic liquefied strength analysis estimates the potential deformations that may result from an eventual loss of strength in the liquefied sand zones. This is a final analysis step to verify that the embankment will remain stable under gravity loads after mobilization of the liquefied strengths. This was accomplished through the following process:

- The motion at the base of the model was stopped after 40 s of earthquake shaking.
- Viscous damping was nominally increased in all zones to 5% of critical.
- The model was solved for an additional 5 s to allow velocities and accelerations to decrease and displacements to stabilize. The viscous damping was then reduced to approximately 2% and modified to include only stiffness proportional damping.
- The maximum r_u in each of the foundation sand elements was compared to the r_u limit of 0.7, which indicates liquefaction. Wherever this r_u limit was exceeded, the element was converted from the UBCSAND model to the Mohr–Coulomb model and the liquefied strength was assigned to that element. A check was made to ensure that the liquefied strength assigned did not exceed the estimate of initial drained strength, which is facilitated by the use of a liquefied strength ratio as suggested by Stark and Mesri (1992). A reduced elastic shear stiffness equal to 10 times the liquefied strength was also assumed in these elements.
- The solution was continued in dynamic mode until the model reached equilibrium and the displacements were no longer increasing.

This process is a proper dynamic solution, but incorporates the assumption that the drop in strength within liquefied elements occurs simultaneously and instantaneously in all of the susceptible elements. It also assumed that applying the liquefied strength to liquefied elements adequately captures any effects of pore-water flow occurring after the end of shaking and (or) void redistribution beneath the fine-grained blanket, and that the available strength is never greater than the liquefied strength estimated using procedures developed from case histories (e.g., Seed and Harder 1990; Stark and Mesri 1992; Olson and Stark 2002). The UBCSAND model also captures the post-liquefaction softening during the earthquake shaking, and the mobilized strength at the end of shaking may be less than the estimated value of liquefied strength.

Idriss and Boulanger (2007) re-evaluated post-liquefaction strengths using case histories analyzed by Stark and Mesri (1992) and Olson and Stark (2002). As suggested by Stark and Mesri (1992), Idriss and Boulanger (2007) present the post-liquefaction strength in the form of a strength ratio so comparison with the strength ratios reported can be made. The post-liquefaction strength ratios applied in the FLAC analyses for the upper foundation sands beneath the dam are lower than the ratios estimated from the Idriss and Boulanger (2007) correlation for the median blowcount. The post-liquefaction strength ratios applied in the FLAC analyses for the upper foundation sands were estimated using Stark and Mesri (1992) and Olson and Stark (2002) and the 33rd-percentile values for blowcount, which is typical for USACE projects (USACE 1970).

Because the liquefied strength is expressed as a strength ratio and the effective stress at the toes of the dam is low, the AP recommended minimum liquefied strengths of 14.8, 16.8, and 28.7 kPa (310, 350, and 600 psf) for the three critical foundation layers: fine-grained blanket, upper foundation sand, and lower foundation sand, respectively. These values were used in the analysis instead of 10.1, 10.5, and 21.6 kPa (210, 220, and 450 psf), which are the values based on a liquefied strength ratio of and the effective vertical stresses at the downstream toe. The liquefied strength ratios used for the three critical foundation layers — fine-grained blanket, upper foundation sand, and lower foundation sand — are 0.141, 0.154, and 0.197, respectively, based on Stark and Mesri (1992) and Olson and Stark (2002). The AP felt values of 10.1, 10.5, and 21.6 kPa (210, 220, and 450 psf) were too low based on comparison with other empirical relationships and experience. Thus, strength ratios derived from Idriss and Boulanger (2007) or other correlations at low effective stresses may lead to somewhat lower liquefied strengths at the downstream toe of the dam because the liquefied strength is expressed as a strength ratio and the effective stress at the toe of the dam is low. The AP also recommended that the lower of the drained strength or the values of 14.8, 16.8, and 28.7 kPa (310, 350, and 600 psf) be used in the analysis.

FLAC analysis results

A summary of key results from the FLAC analyses are provided below. These results include those from the initial static analysis and the seismic analysis of the unremediated dam. A comparison of selected predictions with the observed performance from case histories is also provided to reinforce the conclusions.

Initial stress conditions

The stress state at the start of the seismic analysis was determined via plots of vertical effective stress, horizontal effective stress, horizontal shear stress, and pore pressure (see Fig. 5). These results show the fine-grained blanket beneath the reservoir causes a substantial decrease in hydraulic head. These results are consistent with recent piezometer measurements, which were used to calibrate the hydraulic boundary conditions. The resulting decrease in pore pressure within

the foundation sand leads to a corresponding increase in effective stress. This is significant for the seismic analysis because of the increase in liquefaction resistance that accompanies an increase in effective stress. If the fine-grained blanket is compromised in some manner, the foundation sands may exhibit a higher liquefaction potential and greater seepage.

Liquefaction extent

The potential for liquefaction was evaluated in both the foundation sand and fine-grained blanket. The UBCSAND model generates shear-induced pore pressures in the foundation sand. These pore pressures soften the element, can lead to a stress–strain response controlled by dilation, and are used to determine the elements that will suffer a strength loss to the estimated liquefied strength in the post-dynamic analysis. Liquefaction in the fine-grained blanket produces a softening of the element and a switch from the hyperbolic-hysteretic model to the multi-linear ratchet model (see Fig. 4).

Foundation sands behavior

Liquefaction within the foundation sand is evaluated through contours of maximum pore pressure ratio, r_u, which occurred during the design ground motion. These values may be greater than the r_u value at the end of the ground motion due to the effects of pore pressure dissipation and element dilation. Figure 6 shows the progression of r_u at various times during the design ground motion as well as contours of the maximum r_u generated in the foundation sands during shaking.

The predicted build-up of pore pressures follows a rational trend with a significant amount of pore pressure being generated between 1.0 and 2.0 s. This time period corresponds to the initial large-velocity pulse in the input ground motion. By 5 s, there are high pore pressures consistent with liquefaction in the upper sand layers both upstream and downstream of the dam. Figures 6*b* and 6*c* show elevated pore pressures in the looser sand layers beneath the outer portion of both the upstream and downstream shells. Beneath the downstream slope, the pore pressure ratios increase to a maximum of about 0.7 and then drop by dilation and dissipation to surrounding areas that generate lower pore pressure ratios, e.g., 0.2. Thus, the maximum pore pressure ratio beneath the slope is rather momentary and decreases as the shaking continues. The effects of dissipation are also seen below the downstream toe as pore pressures generated by liquefaction at and near the downstream toe migrate to locations beneath the downstream slope.

The extent of pore pressure generation both upstream and downstream of the dam increases as the shaking continues, leading to almost complete liquefaction of the sands downstream of the dam by the end of the ground motion. The extensive liquefaction downstream of the dam occurs over the full depth of the sand deposit. These high pore pressures and the softened response that results appear to have little impact on the predicted deformations of the dam. The small zone of low pore pressure at each edge of the model is an anomalous boundary effect. Liquefaction upstream of the dam is extensive, but limited to the upper sand layers beneath the fine-grained blanket.

A post-earthquake analysis was performed to evaluate the effect of liquefied strengths as estimated from case histories (Stark and Mesri 1992; Castro 1995; Olson and Stark 2002). These reduced strengths were applied to any zone that experienced even a momentary increase in pore pressure ratio above 0.7. This conservative, but reasonable, interpretation of liquefaction triggering is considered accepted practice, and reflects the presence and importance of the overlying low permeability fine-grained blanket in pore pressure generation. This resulted in the looser sands beneath the downstream shell being assigned a liquefied strength.

Imposing liquefied strengths in the upstream and downstream liquefied elements did not significantly increase the calculated permanent displacements, which are discussed below. A limited amount of additional shear deformation is predicted through the upper liquefied sands. This movement involves the outer portion of the downstream shell including about two-thirds of the berm zone. The maximum local displacement during the post-earthquake analysis is about 0.23 m (0.75 ft) with a maximum displacement within the embankment section of about 0.12 m (0.39 ft).

Fine-grained blanket behavior

Figure 7 shows the predicted extent of liquefaction in the fine-grained blanket. Most of the fine-grained blanket beneath the dam footprint is predicted to liquefy except for a relatively short section near the downstream toe. Liquefaction of the fine-grained blanket corresponds to large excess pore pressures and a significant softening of its stress–strain behavior. Liquefaction is less extensive beneath the reservoir and downstream of the dam, although continuous or near-continuous layers of liquefaction exist outside of the dam footprint. Liquefaction of the fine-grained blanket means that the predicted stress–strain behavior during loading has significantly softened and the loading response is now likely controlled by dilation. Thus, the UBCTOT model has switched from the hyperbolic formulation to the multi-linear or ratcheting behavior.

The predicted shear strength of the fine-grained blanket does not decrease significantly below the peak strength ratio of 0.35. The estimated strength loss in much of the clay layer is less than about 15% of the initial value even when the stiffness has decreased and the liquefaction criterion is satisfied. Figure 7 shows the shaded zones in which the stiffness is reduced. Nonliquefied zones also exhibit reduced stiffness depending on the estimate of excess pore pressure.

Almost the entire fine-grained blanket that liquefies under the embankment triggers within the first 4 s of the ground motion. The portion under the upstream shell triggers earlier in the shaking, mostly between about 1.25 and 1.75 s. This corresponds to the strong velocity peak early in the ground motion. The peak input velocity at the base of the model is 0.37 m (1.2 ft) per second at 1.24 s. Much of the fine-grained blanket beneath the downstream shell liquefies only slightly later, between about 2.0 and 2.25 s. The soft behavior of the shallow liquefied sands appears to limit the strains experienced in the overlying fine-grained layer.

Because liquefaction of much of the fine-grained layer occurs early in the shaking, the significance of the pre-liquefaction (hyperbolic) portion of the cohesive stress–strain model is diminished in this analysis case. The relative importance of the post-liquefaction stress–strain model is likely to increase and the assumptions related to modeling of the stress–strain behavior become significant. The pre-liquefaction response

Fig. 5. Initial stresses and pore-water pressures prior to shaking at Tuttle Creek Dam: (*a*) initial vertical effective stress, σ'_{yy}; (*b*) initial pore pressure, *u*.

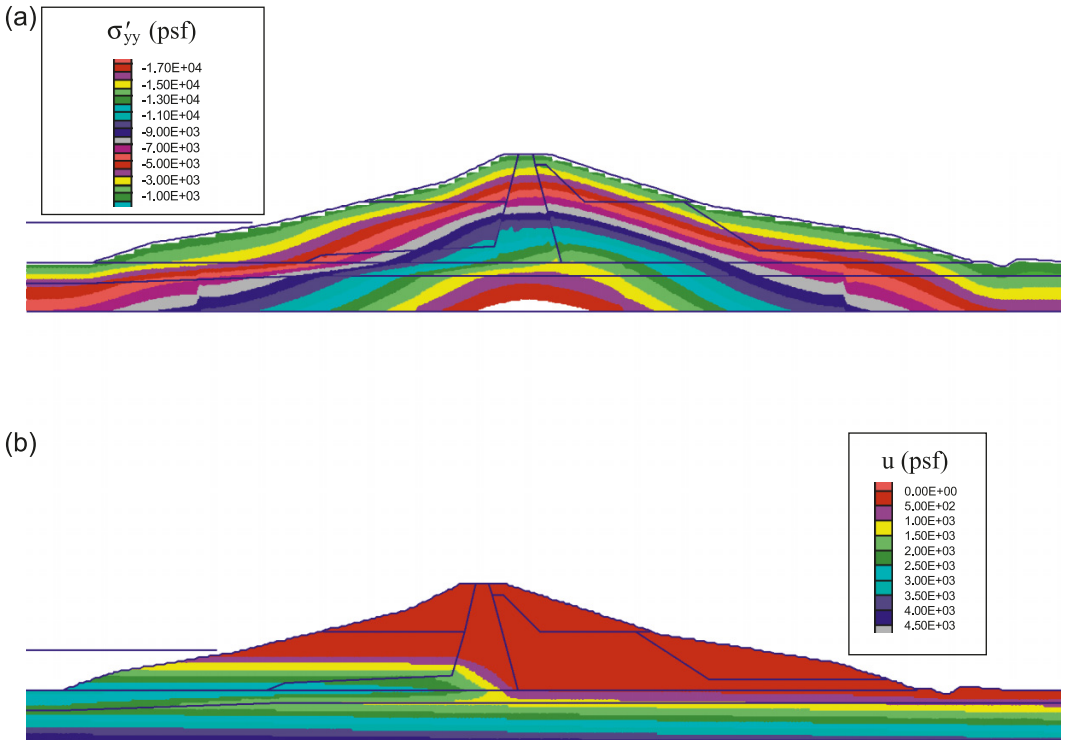

may be more critical for ground motions that do not have a significant early velocity peak.

The loss of undrained strength in the fine-grained blanket is a function of the predicted maximum shear strain as shown in Fig. 3. Many of the final strength ratios are greater than about 0.30 and the strength loss is not continuous under the downstream shell. The predicted loss in strength in much of the fine-grained blanket is less than about 15% of the initial value. This is one of the main differences between this FLAC analysis and prior dynamic analyses performed for the dam. For example, the analysis performed using DYNAFLOW (Popescu 1998) determined practically the same seismic behavior of the middle portion of the embankment as FLAC, but the predicted settlement of the crest was 0.5 m (1.6 ft) and negligible displacements were estimated by FLAC for the upstream and downstream slopes. However, DYNAFLOW predicted significant horizontal displacements of 10 m (30 ft) at the toes, mainly due to nonavailability of the cyclic triaxial test results to calibrate the model. The fine-grained material was modeled as sand with fines, which inherently led to prediction of liquefaction with the associated loss of strength of the foundation blanket. The subsequent TARA-3 and TARA-3FL (Finn and Yogendrakumar 1989) analysis tried to consider the laboratory testing findings within the framework of the model developed for liquefiable sand. Consequently, over 90% of the fine-grained blanket was predicted to mobilize the residual undrained strength ratio of about 0.12 instead of about 0.30.

Liquefaction summary

The results in Figs. 6 and 7 show the extent of liquefaction predicted under Tuttle Creek Dam for the design ground motion. These results can be summarized as follows:

- Limited liquefaction at upstream toe.
- No liquefaction of foundation sand under upstream slope.
- Extensive liquefaction of foundation sand at downstream toe.
- Extensive liquefaction of fine-grained blanket under the dam.

The liquefaction at the downstream toe could result in slope movements that render the downstream relief well system inoperable. As a result, the downstream slope was subsequently remediated to limit the slope movement to a tolerable limit as discussed below.

Earthquake-induced permanent deformations

The predicted evolution of permanent displacement during the design ground motion is shown in Fig. 8 at several locations on the surface of the dam (upstream toe and slope, crest, and downstream slope and toe). The acceleration and velocity histories of the design ground motion are also shown for comparison purposes. The velocity history is often a significant indicator of embankment response as it presents the input motion at a frequency range that is often critical to dam response. Much of the displacement accumulates in a steady and gradual manner over the first 20 s of the design ground motion. This corresponds to the more intense period of shaking as seen on the time history of horizontal input velocity. Displace-

Fig. 6. Foundation sand pore pressure ratio contours at various times: r_u at (*a*) 1.0 s; (*b*) 2.0 s, (*c*) 5.0 s; (*d*) 10.0 s; (*e*) 20.0 s; (*f*) 40.0 s; (*g*) maximum r_u.

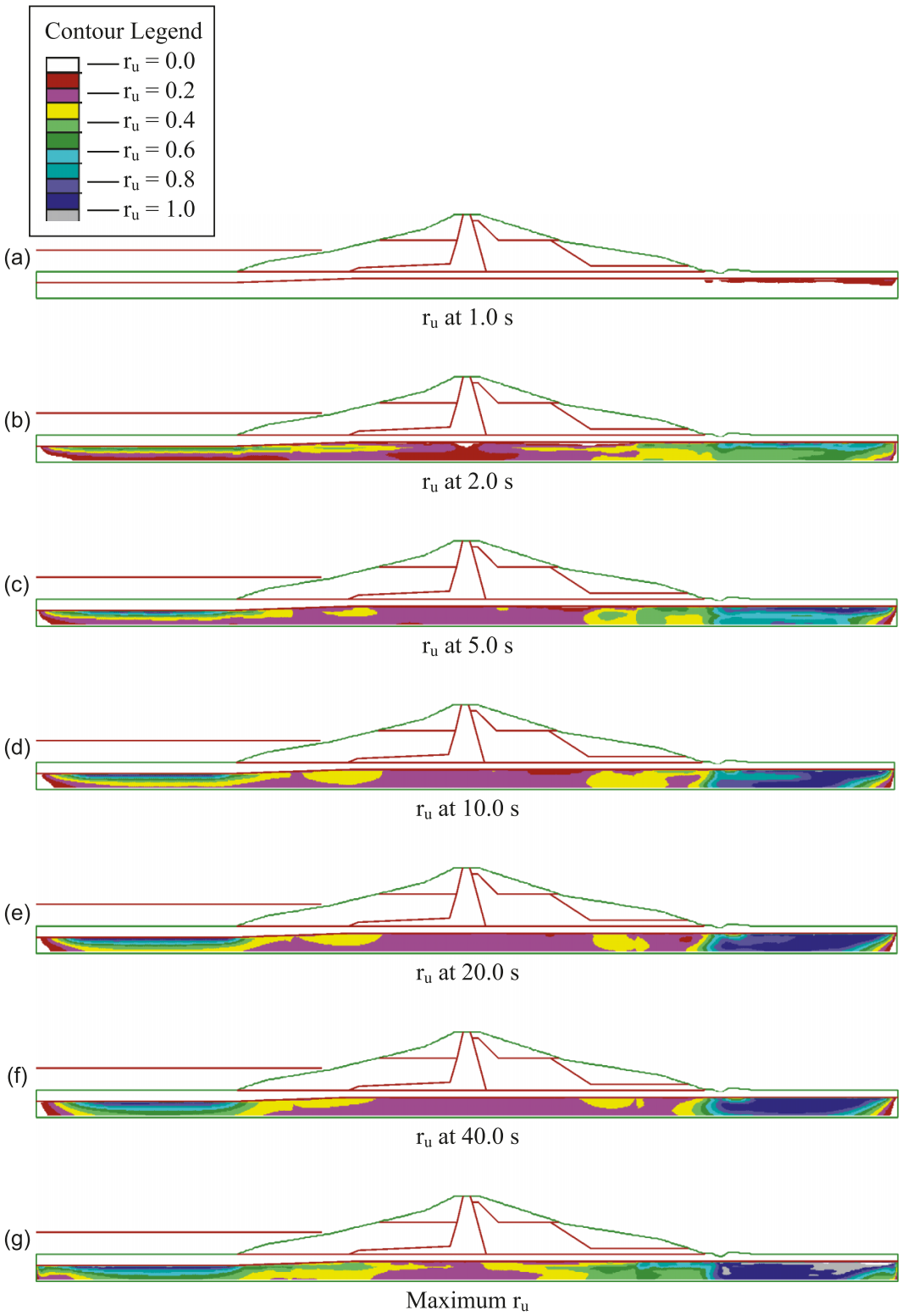

ments at the crest are seen to increase abruptly within the first few seconds of the earthquake, perhaps in response to the strong initial velocity pulse in the ground motion.

Final deformations predicted for the initial unremediated case are relatively modest. The peak displacement vector within the dam footprint at the end of the earthquake motion is only about 0.7 m (2.25 ft) at the downstream toe, with somewhat higher local estimates near the downstream drainage ditch. The crest is predicted to move about 0.04 m (0.12 ft) in the upstream direction with a settlement of about

Fig. 7. Extent of liquefaction within foundation fine-grained blanket.

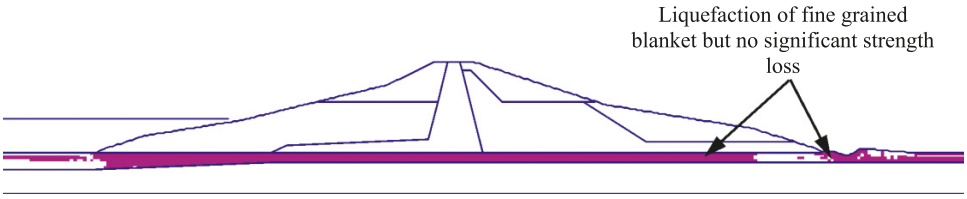

0.55 m (1.75 ft). Figure 8 also shows that the liquefied strength (S_r) was applied in the analysis at an elapsed time of about 45 s.

Parametric studies

A set of parametric studies was performed to evaluate the sensitivity of the predicted permanent deformations to key input parameters. These parametric analyses consist of reanalyzing the base unremediated case after changing one or two input parameters. These studies include reversing the earthquake orientation, using a constant undrained strength ratio of 0.23 within the fine-grained layer, reducing the post-liquefaction stiffness (G_{liq}) of the fine-grained layer by a factor of 5, decreasing the minimum zone height within the fine-grained layer from 3 to 1 ft (1 ft = 0.3048 m), decreasing the bulk modulus of embankment elements by a factor of 5, and modifying the strength and zonation of the upstream shell. These analyses provide a useful set of predictions for evaluating parameter sensitivity.

The general magnitude and distribution of displacements at the end of earthquake shaking are consistent and reasonable between the various parametric analyses. The analyses show relatively modest displacements, with vertical settlements at the crest of 0.55 m (1.75 ft) and a maximum horizontal displacement of the dam near the downstream toe of about 0.7 m (2.25 ft). Two of the parametric studies are described in more detail below.

One parametric analysis involved applying the input ground motion in the opposite (or reverse) direction. Earthquake records often have nonsymmetric characteristics and can sometimes produce significantly different estimates of permanent displacements depending on the orientation of the record. Either orientation is considered to give an equally valid estimate of the embankment response. It is generally appropriate to use the maximum response predicted from the two orientations when evaluating the embankment and foundation rather than the averaged response. In this case, reversing the input motion produced little change in the results.

Reasonably consistent results were also obtained when the fine-grained blanket was modeled in a simpler fashion: the blanket was assumed to be weaker at the start of the earthquake (strength ratio of 0.23 instead of a peak strength ratio of 0.35), but with no additional strength loss with increasing strain. A strength ratioof 0.23 was used because it is a typical or average value observed for many normally consolidated clays in a simple shear mode of shear (Jamiolkowski et al. 1985). The ratio of 0.23 was not degraded because the strength loss from 0.35 to 0.12 did not result in significant deformations in the fine-grained blanket, as shown in Fig. 7 where significant liquefaction of the fine-grained blanket occurs with no significant strength loss.

Strength loss with increasing shear strain in the fine-grained blanket was initially a major concern for the modeling and performance evaluation of Tuttle Creek Dam. However, the parametric study showed that potential strength loss with increasing shear strain in the fine-grained blanket is not a primary factor in the estimated permanent displacements. In addition, the predicted shear strains in the fine-grained blanket were not sufficient to result in a substantial loss of strength over continuous segments of the blanket. For completeness, the relationship between strength in the blanket and embankment deformations was estimated with FLAC as part of the post-liquefaction analysis and produced the following results:

- Assigning the fine-grained blanket an undrained strength ratio of 0.17 resulted in the onset of failure of the lower downstream shell. The primary shear zone extended from the downstream toe to about 38.1 m (125 ft) from the slope toe.
- Assigning the fine-grained blanket an undrained strength ratio of 0.12 resulted in the onset of failure at the upstream toe. This failure is a localized, shallow slip and affects the lower portion of the upstream slope within about 21.3 m (70 ft) of the upstream toe. During this analysis, the downstream failure zone increased in size and extended about 61.1 m (200 ft) from the toe instead of about 38.1 m (125 ft) as described above.
- Assigning the fine-grained blanket an undrained strength ratio of 0.11 resulted in the onset of a large slide in the upstream shell, with the slip surface exiting on the downstream side of the crest and failure of most of the downstream shell beginning.

Thus, if the entire fine-grained blanket mobilizes the residual strength ratio of 0.12, the displacements could be considerably larger than estimated. This sensitivity to a reduction in strength ratio also supported the need for remediation and stabilization of the downstream slope–toe areas.

Comparison of FLAC results with field observations

Comparing numerical analyses to the observed range of actual behavior is an important and useful method for corroborating the general validity of an analysis. Harder (1991), Harder et al. (1998), and Swaisgood (2003) provide useful field observations from prior earthquakes that can be used for this comparison.

Harder (1991) and Harder et al. (1998) summarize recordings of peak transverse crest acceleration from embankment dams and plot this acceleration versus peak transverse acceleration recorded at the base of the dam. This data can be used to estimate whether or not the predicted amplification of the motion by the embankment is appropriate. This graph

Fig. 8. Time histories of surface displacement and horizontal design ground motion: (*a*) horizontal displacements; (*b*) vertical displacements; (*c*) horizontal design motion – acceleration; (*d*) horizontal design motion – velocity. All elevations (El.) in metres. S_r, liquefied strength.

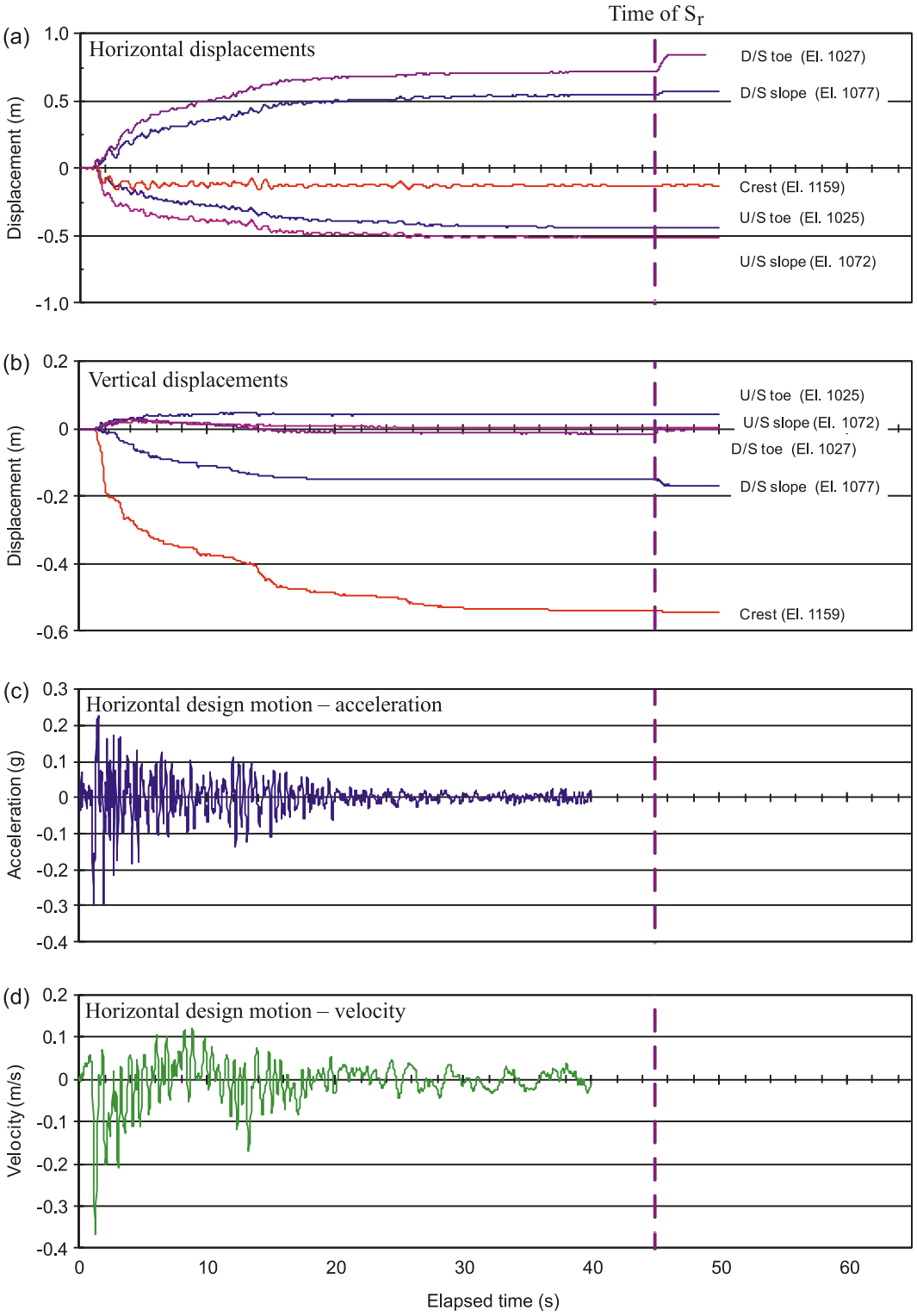

from Harder et al. (1998) is shown in Fig. 9 and superimposed is the peak transverse acceleration from the base and crest of Tuttle Creek Dam estimated using FLAC. The range of calculated accelerations are in agreement with the field observations and plot below the upper bound.

Swaisgood (2003) presents observations of crest settlements due to earthquakes. These settlements are expressed as a percentage of the embankment and foundation height and are related to the peak ground acceleration at the base of the dam. These observations cannot be used directly to confirm

Fig. 9. Comparison of FLAC results and measured field crest accelerations (data from Harder et al. 1998).

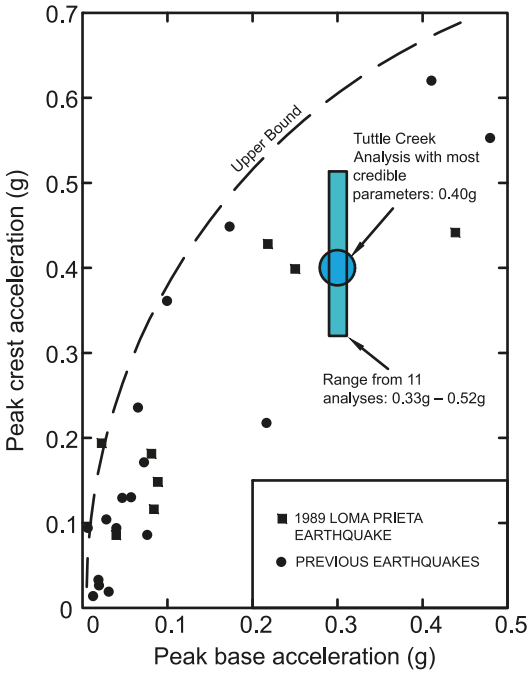

the reasonableness of the FLAC analysis results for Tuttle Creek Dam because case histories believed to involve liquefaction were removed from the database. Because it is reasonable to conclude that the effect of liquefaction at Tuttle Creek Dam will increase the likely displacements, the Swaisgood (2003) relationship still provides a valuable check on the predictions. For example, the FLAC results for Tuttle Creek Dam would be considered unconservative if the predicted displacements were in agreement with the average trend from Swaisgood.

The data collected by Swaisgood (2003) is presented in Fig. 10 where the observed crest settlements are plotted against peak ground acceleration at the base of the dam. The percentage of crest settlement is calculated using the following equation:

$$[2] \qquad \%\,\text{settlement} = \frac{\Delta}{H} \times 100$$

where Δ is the total settlement and H is the height of dam plus the thickness of the alluvium foundation.

Swaisgood (2003) also presents a mathematical relationship between percent crest settlement, PGA, and earthquake magnitude (in surface-wave scale, M_S) as shown below:

$$[3] \qquad \%\,\text{settlement} = e^{(6.07\text{PGA}+0.57M_s-8.00)}$$

The circular data points on Fig. 10 correspond to embankment dams except for those constructed by hydraulic fill techniques. Tuttle Creek Dam was partially built with hydraulic fill, but using a procedure that ensured a high density of the deposited random fill, which was evaluated as nonliquefiable. For Tuttle Creek Dam the design PGA for the design ground motion is 0.3g and is used to plot the Tuttle Creek results in Fig. 10.

Because the Swaisgood (2003) correlation does not address cases with significant liquefaction, the predictions for Tuttle Creek Dam should give significantly smaller crest displacements than predicted by the FLAC analysis. Figure 10 showsthat the observed crest settlements are mostly between 0.04% and 0.5% fora peak ground acceleration of about 0.28g, and between 0.2% and 1.5% for a PGA of 0.56g. Some of the range in observed settlements is due to the different magnitudes of earthquakes included in the database. There are 26 observations from embankment dams with the corresponding earthquake magnitudes ranging from 5.3 to 8.2, with a median of 7.1 and an average of 6.8. The Swaisgood correlation applied to a mean PGA of 0.28g, a dam and foundation thickness of 59.2 m (194 ft), and a magnitude 6.6 earthquake — i.e., Tuttle Creek Dam — suggests a crest settlement of 0.08% or 0.05 m (0.15 ft). When the 84th percentile MCE design PGA of 0.56g is used, the Swaisgood correlation suggests a crest settlement of 0.43% or 0.24 m (0.8 ft).

For Tuttle Creek Dam, the FLAC analysis predicts a crest settlement of 0.5 to 0.7 m (1.6 to 2.3 ft), or about 0.55 m (1.8 ft), for the 84th percentile MCE. This corresponds to a crest settlement of about 1% (0.9 to 1.2%) using the Swaisgood (2003) approach and a dam plus foundation thickness of 59.2 m (194 ft). A crest settlement of about 1% and a PGA of 0.30g plot near the upper bound of the Swaisgood (2003) data. It is not surprising that the Tuttle Creek Dam predictions lie above the best estimate trend from these Swaisgood data because the weak foundation soils cause much of the crest settlement. The triggering of liquefaction in the analysis would also be expected to increase the displacements above those predicted by the Swaisgood correlation. Regardless, a predicted crest settlement of about 0.55 m (1.8 ft) is in agreement with the Swaisgood (2003) data and well below the KCD design criterion of 1.5 m (5.0 ft).

In summary, the predictions of peak crest acceleration and settlement compare reasonably with the range of field observations by Harder et al. (1998) and Swaisgood (2003), respectively.

Discussion and uncertainty of FLAC results

Estimating seismically induced deformations of dams using numerical analysis is a difficult process. The complexity and uncertainty of the analysis is increased substantially by addressing nonlinear soil behavior, the generation of excess pore pressures, and the large changes in constitutive behavior that can occur upon liquefaction. Results from a rigorous and substantiated analysis program can be a useful part of a dam safety evaluation as they often provide valuable insights into the potential behavior of the dam. However, the results should always be evaluated as one part of a more complete framework. This framework includes a thorough knowledge of the dam and properties, the results of previous and (or) more simplified analysis efforts, an understanding of the strengths and limitations of the analysis approach and application, and the observed behavior of similar dams under earthquake loading. For example, displacement predictions from the most ably performed analyses are often considered to be within a factor of 2 of the actual best estimate. The AP

Fig. 10. Comparison of FLAC results and measured field crest settlements (data from Swaisgood 2003).

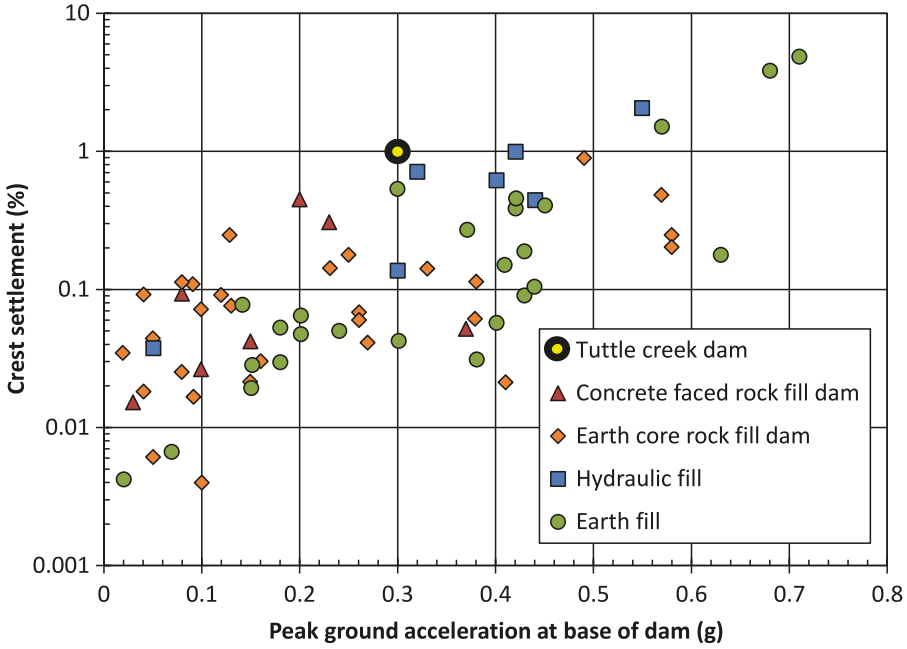

and the KCD considered these factors in their safety evaluation of Tuttle Creek Dam.

The Evaluation Report (USACE 2002*a*, 2002*b*) prepared by the KCD for Tuttle Creek Dam defines the acceptable safety factors and deformations for post-earthquake conditions as

- Factor of safety for post-earthquake limit equilibrium of 1.2 or greater.
- Maximum freeboard loss of 1.5 m (5 ft).
- Maximum horizontal deformation of 0.3 m (1 ft) at the downstream toe.
- Maximum horizontal deformation of 3 m (10 ft) at the upstream toe.

The predicted displacements at the end of the analysis are about 0.55 m (~2 ft) at the upstream toe with a crest settlement of about 0.57 m (~2 ft). Both of these estimates are well within the acceptable deformations defined by the KCD. It was decided that no remedial measures were required for the upstream slope to meet the applicable safety criteria. The predicted displacements at the downstream toe are about 0.7 m (~2.5 ft) with an upper bound of about 1.5 m (5 ft). This displacement magnitude would be acceptable for most embankment dams, however because of the critical role of the downstream toe relief wells, the acceptable displacement criterion for the downstream toe was reduced to 0.3 m (1 ft). The parametric analyses also indicate the potential for much larger displacements in the downstream shell and toe area. These deformations are related to the extent of liquefaction that may occur beneath the outer portion of the downstream shell as well as the amount of strength loss experienced in the fine-grained blanket.

The analyses suggest that additional strength loss in the foundation sands at the downstream toe and the resulting deformations should be considered in the design of remedial measures due to the critical nature of damage to and loss of the pressure relief wells. This consideration is supported by the continuous fine-grained blanket that overlies the foundation sands and can prevent pore pressures from dissipating and contributing to void redistribution. Therefore, these analyses support the need for remediation and stabilization of the downstream slope and toe areas with due consideration for drainage effects.

Summary and conclusions

The FLAC analysis using the calibrated UBCSAND and UBCTOT constitutive models provided valuable insight into the potential performance of an unremediated Tuttle Creek Dam when subjected to the design ground motion. These analyses were used to both understand the seismic performance of the dam and evaluate various remediation schemes. The estimated permanent deformations for the unremediated Tuttle Creek Dam using the design ground motion are as follows:

- Crest settlement of about 0.57 m (~2 ft).
- Permanent deformations at the upstream toe of about 0.55 m (~2 ft).
- Permanent deformations at the downstream toe of about 0.7 m (~2.5 ft), although significantly larger displacements may occur.

These deformations are considered best-estimate values based on the characterization of the foundation and embankment properties. Some uncertainty is expected between analytical predictions and actual behavior, although the general magnitude of the predicted displacements is believed to be a reasonable estimate of embankment performance (i.e., best estimate of actual behavior is likely within a factor of 2). These permanent deformations essentially arise from liquefaction of the foundation sand, especially at the downstream toe, and the accumulated strains and associated softening in the fine-grained blanket.

A comparison of the FLAC results above and the allowable post-earthquake deformations (1.5 m (5 ft) vertically at

the crest, 3 m (10 ft) laterally at the upstream toe, and 0.3 m (1 ft) laterally at the downstream toe) shows that potential movements of the downstream shell are problematic for the design ground motion. Furthermore, the estimated downstream displacements are sensitive to the extent to which liquefaction occurs beneath the downstream section of the dam and could be larger than predicted. As a result, stabilization of the downstream shell and toe was implemented.

The estimated permanent deformation for the upstream toe is less than the allowable post-earthquake deformation criteria and the 25.6 m (84 ft) of existing freeboard was deemed adequate to accommodate the predicted crest settlement of 0.6 m (2 ft). Because of the dam safety risks associated with construction of the cutoff wall and the predicted upstream permanent deformations being only about 0.6 m (~2 ft), the original plans for upstream slope stabilization and a cutoff wall were eliminated. This resulted in a project savings of about US$65 million.

Acknowledgements

A project of this scope requires the contributions of many participants beyond those of the authors. Ms. Cynthia Moses, USACE, Kansas City District, was instrumental in managing the project and Ms. Kathleen Lust of the District administered the construction activities. The authors recognize and appreciate the work of these individuals and many other USACE personnel. Any opinions, findings, and conclusions or recommendations expressed in this paper are those of the authors and do not necessarily reflect the views of the USACE.

References

ASTM. 2006. Standard practice for classification of soils for engineering purposes (Unified Soil Classification System). ASTM standard D2487. American Society for Testing and Materials, West Conshohocken, Pa.

Beaty, M.H. 2001. A synthesized approach for estimating liquefaction-induced displacements of geotechnical structures. Ph.D. thesis, Department of Civil Engineering, The University of British Columbia, Vancouver, B.C. Available from hdl.handle.net/2429/13684 [accessed 3 February 2012].

Boulanger, R.W., and Idriss, I.M. 2006. Liquefaction susceptibility criteria for silts and clays. Journal of Geotechnical and Geoenvironmental Engineering, **132**(11): 1413–1426. doi:10.1061/(ASCE)1090-0241(2006)132:11(1413).

Byrne, P.M., and Seid-Karbasi, M. 2003. Seismic stability of impoundments. *In* Proceedings of the17th Annual Symposium, Vancouver Geotechnical Society, Vancouver, B.C.

Byrne, P.M., Park, S.S., and Beaty, M.H. 2003. Seismic liquefaction: centrifuge and numerical modeling. *In* Proceedings of 3rd International FLAC Symposium, Sudbury.

Byrne, P.M., Park, S.-S., Beaty, M.H., Sharp, M., Gonzalez, L., and Abdoun, T. 2004. Numerical modeling of liquefaction and comparison with centrifuge tests. Canadian Geotechnical Journal, **41**(2): 193–211. doi:10.1139/t03-088.

Castro, G. 1995. Empirical methods in liquefaction evaluation. *In* Proceedings of Primer Ciclo de Conferencias Internacionales Leonardo Zeevaert, Mexico City, November 1995. [In English.]

Castro, G. 1999. Letter report on four triaxial tests on foundation silts. *In* Evaluation Report, Vol. IV, Appendices to Phase II Special Investigations, Part 2: Detailed field investigation and evaluation of repair alternatives: seepage analysis. Vol. IV of VII, Appendix A-4. U.S. Army Corps of Engineers, Kansas City District.

Castro, G. 2000*a*. Letter report on selection of soil parameters for foundation silts. *In* Evaluation Report, Vol. IV, Appendices to Phase II Special Investigations, Part 2: Detailed field investigation and evaluation of repair alternatives: seepage analysis. Vol. IV of VII, Appendix A-5. U.S. Army Corps of Engineers, Kansas City District.

Castro, G. 2000*b*. Letter report on two axial compression and two axial extension tests on foundation silts. *In* Evaluation Report, Volume IV, Appendices to Phase II Special Investigations, Part 2: Detailed field investigation and evaluation of repair alternatives: seepage analysis. Vol. IV of VII, Appendix A-6. U.S. Army Corps of Engineers, Kansas City District.

Castro, G., Walberg, F.C., and Perlea, V. 2003. Dynamic properties of cohesive soil in the foundation of an embankment dam. *In* Proceedings of 21st International Conference on Large Dams (ICOLD), Q.83-R.30, June 2003. Vol. 3, pp. 497–518.

GEI Consultants, Inc. 2000. Report on laboratory testing program on foundation silts. *In* Evaluation Report, Vol. IV, Appendices to Phase II Special Investigations, Part 2: Detailed field investigation and evaluation of repair alternatives: seepage analysis. Vol. IV of VII, Appendix A-6. U.S. Army Corps of Engineers, Kansas City District.

Finn, W.D.L., and Yogendrakumar, M. 1989. TARA-3FL: Program for analysis liquefaction induced flow deformations. Department of Civil Engineering, The University of British Columbia, Vancouver, B.C.

Harder, L.F., Jr. 1991. Performance of earth dams during the Loma Prieta earthquake. *In* Proceedings of the Second International Conference on Recent Advances in Geotechnical Engineering and Soil Dynamics, St. Louis, Mo., 11–15 March 1991. pp. 1673–1680.

Harder, L.F., Jr., Bray, J.D., Volpe, R.L., and Rodda, K.V. 1998. Performance of earth dams during the Loma Prieta earthquake. Professional Paper. U.S. Geological Survey, Reston, Va. Report No. P 1552-D.

Idriss, I.M., and Boulanger, R.W. 2007. SPT- and CPT-based relationships for the residual shear strength of liquefied soils. 2007 Ishihara Lecture. *In* Proceedings of 4th International Conference on Earthquake Geotechnical Engineering, Thessaloniki, Greece, 25–28 June 2007. *Edited by* K.D. Pitilakis. Springer, the Netherlands. Vol. 1, pp. 1–22.

Idriss, I.M., and Boulanger, R.W. 2008. Soil liquefaction during earthquakes. Monograph MNO-12. Earthquake Engineering Research Institute (EERI), Oakland, Calif.

Idriss, I.M., and Sun, J.I. 1992. User's manual for SHAKE91: a computer program for earthquake response analysis of horizontally layered sites. Research Report. Center for Geotechnical Modeling, Department of Civil and Environmental Engineering, University of California, Davis, Calif.

Itasca Consulting Group, Inc. 2000. FLAC – Fast Lagrangian Analysis of Continua. Version 5.0 [computer program]. Itasca Consulting Group, Inc., Minneapolis, Minn.

Jamiolkowski, M., Ladd, C.C., Germaine, J.T., and Lancellotta, R. 1985. New Developments in Field and Laboratory Testing of Soils. *In* Proceedings of the 11th International Conference on Soil Mechanics and Foundation Engineering. Vol. 1, pp. 57–154.

Kokusho, T. 1999. Water film in liquefied sand and its effect on lateral spread. Journal of Geotechnical Engineering, **125**(10): 817–826.

Kokusho, T., and Kojima, T. 2002. Mechanism for postliquefaction water film generation in layered sand. Journal of Geotechnical Engineering, **128**(2): 129–137.

Lane, K.S., and Fehrman, R.G. 1960. Tuttle Creek Dam of rolled shale and dredged sand. Journal of the Soil Mechanics and Foundations Division, ASCE, **86**(SM6): 11–34.

Marcuson, W.F., and Hynes, M.E. 1990. Stability of slopes and embankments during earthquake. *In* Proceedings of the ASCE/ Penn DOT Geotechnical Seminar, Hershey, Pa., 10–11 April 1990.

Marcuson, W.F., III, Ballard, R.F., Jr., and Ledbetter, R.H. 1979. Liquefaction failure of tailings dams resulting from the Near Izu Oshima Earthquake, 14 and 15 January 1978. *In* Proceedings of the 6th Pan-American Conference on Soil Mechanics and Foundation Engineering, Lima, Peru. Vol. 2, pp. 69–80.

Marcuson, W.F., Hynes, M.E., and Franklin, A.G. 1990. Evaluation and use of residual strength in seismic safety analysis of embankments. Earthquake Spectra, **6**(3): 529–572. doi:10.1193/ 1.1585586.

Naesgaard, E., Byrne, P.M., Seid-Karbasi, M., and Park, S.S. 2005. Modeling flow liquefaction, its mitigation, and comparison with centrifuge tests. *In* Proceedings of the Geotechnical Earthquake Engineering Satellite Conference, Osaka, Japan.

Naesgaard, E., Byrne, P.M., and Seid-Karbasi, M. 2006. Modeling flow liquefaction and pore water redistribution mechanisms. *In* Proceedings of he 8th National Conferrence on Earthquake Engineering, San Francisco, Calif.

Olson, S.M., and Stark, T.D. 2002. Liquefied strength ratio from liquefaction flow failure case histories. Canadian Geotechnical Journal, **39**(3): 629–647. doi:10.1139/t02-001.

Perlea, V.G. 2006. Draft memorandum, April 17: Tuttle Creek Dam, summary of soil properties for use in FLAC analysis. U.S. Army Corps of Engineers, Kansas City District.

Popescu, R. 1998. Evaluation report, Appendix V, Phase II Special Investigations, Part 2: Detailed field investigation and evaluation of repair alternatives: seepage analysis, Appendix F "DYNA-FLOW Analysis", Volume V. U.S. Army Corps of Engineers, Kansas City District.

Seed, R.B., and Harder, L.F. 1990. SPT-based analysis of cyclic pore pressure generation and undrained residual strength. *In* Proceedings of the H.B. Seed Memorial Symposium. Bi-Tech Publishing Ltd., Richmond, B.C. Vol. 2, pp. 351–376.

Seed, H.B., Lee, K.L., Idriss, I.M., and Makdisi, F.I. 1975. The slides in the San Fernando Dams during the earthquake of February 9, 1971. Journal of the Soil Mechanics and Foundation Engineering Division, ASCE, **101**(GT7): 651–688.

Seid-Karbasi, M., Byrne, P.M., Naesgaard, E., Park, S.S., Wijewickreme, D., and Phillips, R. 2005. Response of sloping ground with liquefiable materials during an earthquake: a class A prediction. *In* Proceedings of the 11th International Conference, International Association for Computer Methods and Advances in Geomechanics, Italy.

Somerville, P., Walberg, F.C., and Perlea, V.G. 2003. Seismic hazard analysis and selection of design earthquake for a dam in Kansas. *In* Proceedings of the 21st International Conference on Large Dams (ICOLD), Q.83 – R.29, June, Vol. 3, pp. 473–495.

Stark, T.D., and Mesri, G. 1992. Undrained shear strength of liquefied sands for stability analyses. Journal of Geotechnical Engineering, **118**(11): 1727–1747. doi:10.1061/(ASCE)0733-9410(1992)118:11(1727).

Swaisgood, J.R. 2003. Embankment dam deformations caused by earthquakes. *In* Proceedings of the 2003 Pacific Conference on Earthquake Engineering. Paper No. 014.

USACE. 1970. Engineering and design: stability of earth and rock-fill dams. Department of the Army Corps of Engineers, Office of the Chief of Engineers, Washington, D.C. Report No. EM 1110-2-1902, 1 April 1970,

USACE. 1998. Evaluation Report, Phase II Special Investigations: Seepage Analysis; Liquefaction Analysis. U.S. Army Corps of Engineers, Kansas City District. [Unpublished.]

USACE. 1999. Evaluation Report, Phase II Special Investigations: Seismological Investigation. U.S. Army Corps of Engineers, Kansas City District. [Unpublished.]

USACE. 2002*a*. Evaluation Report, Phase II Special Investigations: Slope Stability Analysis. U.S. Army Corps of Engineers, Kansas City District. [Unpublished.]

USACE. 2002*b*. Evaluation Report, Phase II Special Investigations: Seismic Deformation Analysis. U.S. Army Corps of Engineers, Kansas City District. [Unpublished.]

USACE. 2007. Tuttle Creek Dam: Foundation Modification Project: Downstream Stabilization and Buried Collector System. 95% Submittal, Plans and Specifications. U.S. Army Corps of Engineers, Kansas City District.

Yang, D., Naesgaard, E., Byrne, P.M., Adalier, K., and Abdoun, T. 2004. Numerical model verification and calibration of George Massey Tunnel using centrifuge models. Canadian Geotechnical Journal, **41**(5): 921–942. doi:10.1139/t04-039.

Youd, T.L., Idriss, I.M., Andrus, R.D., Arango, I., Castro, G., Christian, J.T., et al. 2001. Liquefaction resistance of soils: summary report from the 1996 NCEER and 1998 NCEER/NSF workshops on evaluation of liquefaction resistance of soils. Journal of Geotechnical and Geoenvironmental Engineering, **127** (10): 817–833. doi:10.1061/(ASCE)1090-0241(2001)127:10 (817).